

Renormalization-group improved Higgs to two gluons decay rate

Gauhar Abbas^{a1}
 Astha Jain^{a2}
 Vartika Singh^{a3}
 Neelam Singh^{a4}

^a Department of Physics, Indian Institute of Technology (BHU), Varanasi 221005, India

Abstract

We investigate the renormalization-group scale and scheme dependence of the $H \rightarrow gg$ decay rate at the order $N^4\text{LO}$ in the renormalization-group summed perturbative theory, which employs the summation of all renormalization-group accessible logarithms including the leading and subsequent four sub-leading logarithmic contributions to the full perturbative series expansion. Moreover, we study the higher-order behaviour of the $H \rightarrow gg$ decay width using the asymptotic Padé approximant method in four different renormalization schemes. Furthermore, the higher-order behaviour is independently investigated in the framework of the asymptotic Padé-Borel approximant method where generalized Borel-transform is used as an analytic continuation of the original perturbative expansion. The predictions of the asymptotic Padé-Borel approximant method are found to be in agreement with that of the asymptotic Padé approximant method. Finally, we provide the $H \rightarrow gg$ decay rate at the order $N^5\text{LO}$ in the fixed-order $\Gamma_{N^5\text{LO}} = \Gamma_0(1.8375 \pm 0.047_{\alpha_s(M_Z),1\%} \pm 0.0004_{M_t} \pm 0.0066_{M_H} \pm 0.0036_P \pm 0.007_s \pm 0.0005_{sc})$, and $\Gamma_{\text{RGSN}^5\text{LO}} = \Gamma_0(1.841 \pm 0.047_{\alpha_s(M_Z),1\%} \pm 0.0005_{M_t} \pm 0.0066_{M_H} \pm 0.0002_\mu \pm 0.0027_P \pm 0.001_{sc})$ in the renormalization-group summed perturbative theories.

¹email: gauhar.phy@iitbhu.ac.in

²email: astha.jain.phy16@itbhu.ac.in

³email: vartikasingsh.rs.phy19@itbhu.ac.in

⁴email: neelamsingh.rs.phy19@itbhu.ac.in

1 Introduction

The discovery of the Higgs boson at the Large Hadron Collider (LHC) is the first step towards a better understanding of the electroweak symmetry breaking of the standard model (SM) [1, 2]. Moreover, studying the phenomenological behaviour of this particle is immensely important for providing crucial information for physics beyond the SM. In the SM, the Higgs boson dominantly decays to a pair of bottom quarks, that is, $H \rightarrow \bar{b}b(+\text{hadrons})$ followed by the second leading hadronic decay channel $H \rightarrow gg$, which is predominantly mediated by the top quark.

There has been an extensive theoretical investigation of the decay $H \rightarrow gg$ in literature [3, 4, 5]. For instance, it has been computed in an effective theory approach by considering $M_H \ll 2m_t$ in reference [6]. The $1/m_t$ corrections are evaluated up to N²LO in references [7, 8]. The effective Higgs coupling to gluons is computed up to N⁴LO in references [9, 10, 11, 12, 13, 14, 15], up to N³LO in the limit of heavy top quarks in references [16, 17, 18], and up to NLO with the full quark mass dependence in references [19, 20]. The subleading finite top-quark mass effects in the large top mass expansion are known at N²LO [21], and the top-bottom interference at NLO accuracy is computed in reference [22, 23].

We observe that a low energy theorem can also yield the QCD corrections to the $H \rightarrow gg$ decay width at N⁴LO in the heavy quark limit [3, 24]. The effective Higgs-gluons Lagrangian in the heavy top-quark limit in this approach is derived by keeping the terms that depend only on the Higgs field, and using the transformation of the gluonic field strength operator and the strong coupling constant from $n_f + 1$ to n_f flavours [25, 26].

The absorptive part of the corresponding vacuum polarization is computed up to N²LO in references [6, 27, 28]. The N³LO corrections to the absorptive part have been obtained in references [29, 30, 31, 32]. Moreover, the $H \rightarrow gg$ decay rate is computed in the limit of a heavy top quark and any number of massless light flavours at N⁴LO in reference [33]. The new theoretical development in this work is the computation of the absorptive part of the corresponding vacuum polarization at the order N⁴LO, which was missing so far. The computed correction to the $H \rightarrow gg$ decay rate at N⁴LO is slightly smaller than the $1/m_{top}$ effect at N²LO, and larger than the presently unknown $1/m_{top}$ effect at N³LO [33]. Moreover, this computation has reduced the uncertainty due to the truncation of the perturbation series, thus providing an improvement in the $H \rightarrow gg$ decay rate.

The hadronic processes such as $H \rightarrow gg$ are usually calculated up to finite order within perturbative QCD. Therefore, these calculations are plagued by a significant dependence on the renormalization (RG) scale parameter μ . There are several prescriptions for dealing with this dependence in literature so that a physical prediction can be obtained. For instance, this scale in practice, can be identified with the mass of the decaying particle. One possibility is to use a value of μ such that the known calculated terms in perturbation expansion show a local insensitivity to this value. In addition, a value of μ may also be chosen, which minimizes the highest-order known term of the perturbative expansion [34]. It is obvious that using different prescriptions may cause theoretical uncertainty in a prediction. The ambiguity arising due to the RG scale dependence in $H \rightarrow gg$ decay at the order N⁴LO is of particular interest for the precision physics within the SM as well as beyond the SM physics [34, 35, 36, 37].

We note that the renormalization group equation (RGE) is extensively used as a tool to improve the behaviour of the perturbative expansions, and extend their domain of applicability in perturbative quantum field theory. For instance, if the perturbative expansion is known to k -subleading orders, the renormalization group equation can be used to sum the leading and subsequent $(k - 1)$ subleading log contributions to the full perturbative expansion. Such logarithms are known as “RG-accessible” in literature [38, 39].

In this work, we discuss the closed-form summation of these RG-accessible logarithms for the $H \rightarrow gg$ decay rate in the so-called “renormalization-group summed perturbation theory” (RGSPT) in the four different RG schemes, namely, $\overline{\text{MS}}$, SI, OS, and miniMOM. Perturbative series in the RGSPT is expanded in terms of coupling constant and logarithms such that coefficient of every such term can be determined through RG-invariance in terms of its leading coefficient. This is a generalization of the method of the leading logarithm summation and provides the RG-summed perturbative expansion of the series to any given order of the perturbation theory. One of the salient features of the new RGSPT expansions is the reduced sensitivity to RG scale μ in spite of the presence of large logarithms [38].

In literature, RGE is found to be helpful in the extraction of the divergent parts of the bare parameters using the determination of higher-order terms [40, 41]. However, the incorporation of all available higher-order RG-accessible terms to a given order in perturbation theory was first discussed by Maxwell to deal with unphysical

RG scale dependence [42]. This was further applied to moments of QCD lepto-production structure functions, and to N²LO correlation functions for the summation of the leading logarithms in references [43, 44]. This formalism is also used by McKeon to extract one-loop RG functions of ϕ^4 - and ϕ^6 -field theories by performing the summation of leading logarithms to all orders [45]. The summation procedure of McKeon was extended to study the semileptonic B -decay rate in reference [38].

The RGSPT expansions have been employed in various decays and observables in literature, and are shown to exhibit a remarkable improvement in the sensitivity to the renormalization scale. For instance, these are used to study the e^+e^- hadronic cross-section [39], extraction of the strong coupling constant from the hadronic width of the τ -decays [46, 47], extraction of the strange quark mass from moments of the τ -decay spectral function [48] and investigate the QCD static energy at the four-loop in reference [49]. Moreover, RGSPT expansions can further be improved by the method of conformal mapping [46, 47, 50, 51, 52, 53, 54, 55].

In addition to the RG improvement of the $H \rightarrow gg$ decay rate, we also investigate the higher-order behaviour of the perturbative expansion of the $H \rightarrow gg$ decay rate using the asymptotic Padé approximant (APAP) method [56, 57, 58, 59, 60, 61, 62, 63, 64]. Moreover, the higher-order estimate of the beta and gamma function coefficients are also discussed using the same method. These predictions are further independently obtained through the asymptotic Padé-Borel approximant (PBA) method, which provides an additional test of the asymptotic Padé approximant predictions.

Our paper will be presented along the following track: We first briefly review the theoretical formalism, and state-of-the-art computation of the $H \rightarrow gg$ decay rate at N⁴LO in section 2. This is followed by section 3 where we discuss the $H \rightarrow gg$ decay width in the standard “fixed-order perturbation theory” (FOPT), and extract the expansion coefficients in various RG schemes. In section 4, we discuss the $H \rightarrow gg$ decay rate in the RGSPT at N⁴LO. The expansion functions of the RGSPT are derived in an analytic closed-form by solving the differential equation using the method of iteration in this section. We present a thorough discussion of the scale and scheme dependence of the $H \rightarrow gg$ decay rate at N⁴LO in the FOPT in section 5. This is followed by the discussion of scale and scheme dependence of the $H \rightarrow gg$ decay rate at N⁴LO in the RGSPT in section 6. The higher-order behaviour of the $H \rightarrow gg$ decay rate using the APAP formalism is discussed in section 7. The study of the higher-order corrections to the $H \rightarrow gg$ decay rate in the framework of the PBA is presented in section 8. We determine the $H \rightarrow gg$ decay width using the FOPT and the new RGSPT expansions discussed in this work in section 9 in the $\overline{\text{MS}}$, scale invariant (SI), on shell (OS), and the minimal momentum subtraction (miniMOM) schemes. We summarize our results in section 10.

2 Inclusive decay of the Higgs-boson to gluons

In this section, we briefly review the calculation of the inclusive decay of the Higgs-boson to two gluons. The inclusive decay of the Higgs-boson to gluons is calculated in the limit of a large top-quark mass with effectively massless n_f flavours using the following effective Lagrangian [6, 28],

$$\mathcal{L}_{\text{eff}} = \mathcal{L}_{\text{QCD}(n_f)} - 2^{1/4} G_F^{1/2} C_1 H G_a^{\mu\nu} G_{\mu\nu}^a, \quad (2.1)$$

where H represents the Higgs field, the renormalized gluon field-strength tensor is denoted by $G_a^{\mu\nu}$ with n_f flavours, the Lagrangian $\mathcal{L}_{\text{QCD}(n_f)}$ is the QCD Lagrangian, the renormalized coefficient C_1 parametrizes the top-mass dependence, and G_F is the Fermi coupling constant.

The partial decay width of the Higgs-boson to gluons $\Gamma_{H \rightarrow gg}$ decay can be computed using the imaginary part of the Higgs-boson self-energy and written as,

$$\Gamma_{H \rightarrow gg} = \frac{\sqrt{2} G_F}{M_H} |C_1|^2 \text{Im} \Pi^{GG}(-M_H^2 - i\delta), \quad (2.2)$$

where M_H is the mass of the Higgs boson, Π^{GG} represents the contribution to the self-energy of the Higgs boson due to its effective coupling to gluons, and δ is a positive real parameter, which is infinitesimally small.

The coefficient C_1 is known up to N⁴LO and its perturbative expansion is given by,

$$C_1 = -\frac{1}{3} a_s \left(1 + \sum_{n=1} c_n a_s^n(\mu^2) \right), \quad (2.3)$$

where $a_s \equiv \frac{\alpha_s^{n_f}}{4\pi}$ where n_f are number of light flavours.

The known expansion coefficients c_n in the SI scheme at the renormalization scale $\mu = \mu_t$, where $\mu_t = m_t(\mu_t)$ is the $\overline{\text{MS}}$ top quark mass evaluated at scale μ_t , in the $\overline{\text{MS}}$ and OS schemes are written as[33],

$$\begin{aligned}
c_1 &= 11, \quad c_2 = 154.278 + 19L_t + (-11.1667 + 5.33333L_t)n_f, \\
c_{3,\text{SI}} &= 3031.7 + 537.111L_t + 209L_t^2 + (-492.139 + 107.852L_t + 46L_t^2)n_f \\
&\quad + (-14.1255 + 2.85185L_t - 3.55556L_t^2)n_f^2 \\
c_{4,\text{SI}} &= 79815.7 + 12340.2L_t + 9831.33L_t^2 + 2299L_t^3 \\
&\quad + (-15966.1 - 1482.59L_t + 1394.11L_t^2 + 366.667L_t^3)n_f \\
&\quad + (413.572 - 621.891L_t - 94.5741L_t^2 - 69.7778L_t^3)n_f^2 \\
&\quad + (-8.79068 + 23.7531L_t - 2.85185L_t^2 + 2.37037L_t^3)n_f^3 \\
c_{3,\overline{\text{MS}}} &= c_{3,\text{SI}} - 152L_t - 42.6667L_t n_f \\
c_{4,\overline{\text{MS}}} &= c_{4,\text{SI}} - 5576.22L_t - 4230.67L_t^2 + (-1158.59L_t - 934.222L_t^2)n_f + (-5.03704L_t + 71.1111L_t^2)n_f^2 \\
c_{3,\text{OS}} &= c_{3,\text{SI}} + 202.667 + 56.8889n_f \\
c_{4,\text{OS}} &= c_{4,\text{SI}} + 13362.3 + 6688L_t + (2659.9 + 1472L_t)n_f + (-147.307 - 113.778L_t)n_f^2,
\end{aligned} \tag{2.4}$$

where $L_t = \ln(\mu^2/m_t^2)$, μ is the RG scale and m_t is the definition of the top quark mass in the corresponding RG scheme.

The absorptive part of the vacuum polarization is computed at N⁴LO in reference [33], thus, making the Higgs-boson to gluons decay width complete at the N⁴LO order. The absorptive part of the vacuum polarization is written in the following form,

$$\frac{4\pi}{N_A q^4} \text{Im} \Pi^{GG}(q^2) \equiv G(q^2) = 1 + \sum_{n=1} g_n a_s^n, \tag{2.5}$$

where $N_A = 8$ in QCD.

The coefficients g_n of the renormalization of the absorptive part in the $\overline{\text{MS}}$ scheme corresponding to the self-energy of the Higgs boson up to N⁴LO are [33],

$$\begin{aligned}
g_1 &= 73 - \frac{14}{3}n_f - \frac{46}{3}L_q \\
g_2 &= 3887.57 - 629.982n_f + 14.4283n_f^2 - \left[23 \left(73 - \frac{14}{3}n_f \right) + \frac{464}{3} \right] L_q + \frac{529}{3}L_q^2 \\
g_3 &= 163394 - 49409.6n_f + 2974.39n_f^2 - 34.4213n_f^3 - \left[\frac{9769}{9} + \frac{580}{3} \left(73 - \frac{14}{3}n_f \right) \right. \\
&\quad \left. - \frac{92}{3} \left(3887.57 - 629.982n_f + 14.4283n_f^2 \right) \right] L_q + \left[\frac{34684}{9} + \frac{1058}{3} \left(73 - \frac{14}{3}n_f \right) \right] L_q^2 - \frac{48668}{27}L_q^3 \\
g_4 &= 5.45154 \times 10^6 - 2.81728 \times 10^6 n_f + 318324.n_f^2 - 9921.43n_f^3 + 64.359n_f^4 + \left[-38609.3 \right. \\
&\quad \left. - 232 \left(3887.57 - 629.982n_f + 14.4283n_f^2 \right) - \frac{115}{3} \left(163394. - 49409.6n_f + 2974.39n_f^2 - 34.4213n_f^3 \right) \right. \\
&\quad \left. - \frac{68383}{54} \left(73 - \frac{14}{3}n_f \right) \right] L_q + \left[\frac{3924805}{81} + \frac{57362}{9} \left(73 - \frac{14}{3}n_f \right) + \frac{5290}{9} \left(3887.57 - 629.982n_f \right. \right. \\
&\quad \left. \left. + 14.4283n_f^2 \right) \right] L_q^2 + \left[\frac{5093212}{81} - \frac{121670}{27} \left(73 - \frac{14}{3}n_f \right) \right] L_q^3 + \frac{1399205}{81}L_q^4,
\end{aligned} \tag{2.6}$$

where $L_q = \ln\left(\frac{q^2}{\mu^2}\right)$.

The logarithm in equation 2.6 can also be written in terms of the pole mass of the top quark by defining,

$$L_q = T - \ln\left(\frac{\mu^2}{M_t^2}\right), \quad (2.7)$$

where $T \equiv \ln(M_H^2/M_t^2)$ and M_t is the pole mass of the top quark, where we have set $q^2 = M_H^2$.

3 Fixed-order-perturbation theory

In the RGSPT, predicting RG-accessible next-order coefficients becomes more effective if we express the perturbative expansion in terms of the running fermion mass [37]. Therefore, we rewrite the $H \rightarrow gg$ decay rate expansion in terms of the running top-quark mass. For this purpose, we use the relation between the running and pole mass [65, 66],

$$\begin{aligned} \frac{m(\mu)}{M} = & 1 + \left[-1 - \frac{4}{3}l_{\mu M}\right] x(\mu) \\ & + \left[-14.3444 - \frac{445}{72}l_{\mu M} - \frac{19}{24}l_{\mu M}^2 + \left(1.04137 + \frac{13}{36}l_{\mu M} + \frac{1}{12}l_{\mu M}^2\right) n_f\right] x(\mu)^2 \\ & + \left[-198.707 - 78.9409l_{\mu M} - \frac{11779}{864}l_{\mu M}^2 - \frac{475}{432}l_{\mu M}^3 + \left(26.9239 + 12.3257l_{\mu M}\right.\right. \\ & \left.\left. + \frac{911}{432}l_{\mu M}^2 + \frac{11}{54}l_{\mu M}^3\right) n_f + \left(-0.652692 - 0.380301l_{\mu M}^2 - \frac{1}{108}l_{\mu M}^3\right) n_f^2\right] x(\mu)^3, \end{aligned} \quad (3.8)$$

where $l_{\mu M} = \ln \mu^2/M^2$, $x(\mu) = \frac{\alpha_s^{n_f}(\mu)}{\pi}$ and n_f are number of active flavours.

Using above relation, the logarithm L_q in the equation 2.7 can be expressed in terms of $\ln\frac{\mu^2}{m_t^2(\mu)}$. This can be done by writing the logarithm $\ln\left(\frac{\mu^2}{M_t^2}\right)$ as,

$$\begin{aligned} \ln\left(\frac{\mu^2}{M_t^2}\right) = & \ln\frac{\mu^2}{m_t^2(\mu)} + 2x^{(n_f)}(\mu) \left[-1.33333 - \ln\frac{\mu^2}{m_t^2(\mu)}\right] \\ & + 2x^{(n_f)}(\mu)^2 \left[-12.5666 + 1.04137n_f + \left(-5.51389 + 0.361111n_f\right) \ln\frac{\mu^2}{m_t^2(\mu)}\right. \\ & \left. + \left(-1.29167 + 0.0833333n_f\right) \left(\ln\frac{\mu^2}{m_t^2(\mu)}\right)^2\right] + 2x^{(n_f)}(\mu)^3 \left[-173.452 + 25.2666n_f - 0.652691n_f^2\right. \\ & \left. + \left(-70.3593 + 11.9597n_f\right) \ln\frac{\mu^2}{m_t^2(\mu)} + \left(-14.4525 + 2.08102n_f - 0.380301n_f^2\right) \left(\ln\frac{\mu^2}{m_t^2(\mu)}\right)^2\right. \\ & \left. + \left(-2.22454 + 0.287037n_f - 0.00925926n_f^2\right) \left(\ln\frac{\mu^2}{m_t^2(\mu)}\right)^3\right]. \end{aligned} \quad (3.9)$$

Thus, the decay width of $H \rightarrow gg$ acquires the following form in terms of the running top quark mass,

$$\Gamma = \left[\sqrt{2}G_F M_H^3/72\pi\right] x^2(\mu) S[x(\mu), L(\mu)], \quad (3.10)$$

where the perturbative expansion $S[x(\mu), L(\mu)]$ in the FOPT is written as,

$$S_{\text{FOPT}}[x(\mu), L(\mu)] = \sum_{n=0}^{\infty} \sum_{k=0}^n T_{n,k} x^n L^k. \quad (3.11)$$

We work with $n_f = 5$ flavours in this work. The coefficients of expansion $T_{n,k}$ in the $\overline{\text{MS}}$ scheme are,

$$\begin{aligned}
T_{0,0}^{\overline{\text{MS}}} &= 1, T_{1,0}^{\overline{\text{MS}}} = 17.9167 - 3.83333 T, T_{1,1}^{\overline{\text{MS}}} = 3.83333, T_{2,0}^{\overline{\text{MS}}} = 146.586 - 102.146 T + 11.0208 T^2, \\
T_{2,1}^{\overline{\text{MS}}} &= 100.188 - 22.0417 T, T_{2,2}^{\overline{\text{MS}}} = 11.0208, T_{3,0}^{\overline{\text{MS}}} = 123.647 - 1156.52 T + 394.514 T^2 - 28.1644 T^3 \\
T_{3,1}^{\overline{\text{MS}}} &= 1034.83 - 766.826 T + 84.4931 T^2, T_{3,2}^{\overline{\text{MS}}} = 376.545 - 84.4931 T, T_{3,3}^{\overline{\text{MS}}} = 28.1644, \\
T_{4,0}^{\overline{\text{MS}}} &= -11815.8 - 2506.94 T + 5777.77 T^2 - 1274.79 T^3 + 67.4771 T^4, \\
T_{4,1}^{\overline{\text{MS}}} &= 45.6137 - 10430.6 T + 3718.31 T^2 - 269.908 T^3, T_{4,2}^{\overline{\text{MS}}} = 4609.02 - 3615.6 T + 404.863 T^2, \\
T_{4,3}^{\overline{\text{MS}}} &= 1184.31 - 269.908 T, T_{4,4}^{\overline{\text{MS}}} = 67.4771,
\end{aligned} \tag{3.12}$$

and the logarithm is $L(\mu) = \ln(\mu^2/m_t^2(\mu))$.

We can also write the FOPT expansion in terms of SI, OS, and miniMOM schemes. For this purpose, we write equation 2.6 in terms of the SI, OS, and miniMOM mass of the top quark,

$$L_q = T - \ln\left(\frac{\mu^2}{M_{t_p}^2}\right), \tag{3.13}$$

where $T \equiv \ln\left(M_H^2/M_{t_p}^2\right)$ and p stands for SI, OS or miniMOM scheme. In the SI scheme, the coefficients of the FOPT expansion are,

$$\begin{aligned}
T_{0,0}^{\text{SI}} &= 1, T_{1,0}^{\text{SI}} = 17.9167 - 3.83333 T, T_{1,1}^{\text{SI}} = 3.83333, T_{2,0}^{\text{SI}} = 156.808 - 102.146 T + 11.0208 T^2, \\
T_{2,1}^{\text{SI}} &= 107.854 - 22.0417 T, T_{2,2}^{\text{SI}} = 11.0208, T_{3,0}^{\text{SI}} = 452.461 - 1215.3 T + 394.514 T^2 - 28.1644 T^3, \\
T_{3,1}^{\text{SI}} &= 1337.74 - 810.91 T + 84.4931 T^2, T_{3,2}^{\text{SI}} = 427.337 - 84.4931 T, T_{3,3}^{\text{SI}} = 28.1644, \\
T_{4,0}^{\text{SI}} &= -6502.1 - 4935.46 T + 6003.09 T^2 - 1274.79 T^3 + 67.4771 T^4, \\
T_{4,1}^{\text{SI}} &= 6041.54 - 12666.6 T + 3887.29 T^2 - 269.908 T^3, T_{4,2}^{\text{SI}} = 6947.57 - 3992.14 T + 404.863 T^2, \\
T_{4,3}^{\text{SI}} &= 1400.62 - 269.908 T, T_{4,4}^{\text{SI}} = 67.4771.
\end{aligned} \tag{3.14}$$

In a similar manner, we write the coefficients of expansion in the OS scheme,

$$\begin{aligned}
T_{0,0}^{\text{OS}} &= 1, T_{1,0}^{\text{OS}} = 17.9167 - 3.83333 T, T_{1,1}^{\text{OS}} = 3.83333, T_{2,0}^{\text{OS}} = 156.808 - 102.146 T + 11.0208 T^2, \\
T_{2,1}^{\text{OS}} &= 107.854 - 22.0417 T, T_{2,2}^{\text{OS}} = 11.0208, T_{3,0}^{\text{OS}} = 467.684 - 1215.3 T + 394.514 T^2 - 28.1644 T^3, \\
T_{3,1}^{\text{OS}} &= 1337.74 - 810.91 T + 84.4931 T^2, T_{3,2}^{\text{OS}} = 427.337 - 84.4931 T, T_{3,3}^{\text{OS}} = 28.1644, \\
T_{4,0}^{\text{OS}} &= -6091.71 - 4993.81 T + 6003.09 T^2 - 1274.79 T^3 + 67.4771 T^4, \\
T_{4,1}^{\text{OS}} &= 6187.42 - 12666.6 T + 3887.29 T^2 - 269.908 T^3, T_{4,2}^{\text{OS}} = 6947.57 - 3992.14 T + 404.863 T^2, \\
T_{4,3}^{\text{OS}} &= 1400.62 - 269.908 T, T_{4,4}^{\text{OS}} = 67.4771.
\end{aligned} \tag{3.15}$$

We also investigate the Higgs to gluon decay width in the miniMOM version of the OS scheme [67, 68]. In this scheme, the strong coupling is fixed by the knowledge of the gluon and ghost propagators [67, 68]. The expansion coefficients for this scheme can be written using the expansion given in reference [33],

$$\begin{aligned}
T_{0,0}^{\text{MM}} &= 1, T_{1,0}^{\text{MM}} = 13.6528 - 3.83333 T, T_{1,1}^{\text{MM}} = 3.83333, T_{2,0}^{\text{MM}} = 46.9335 - 83.3368 T + 11.0208 T^2, \\
T_{2,1}^{\text{MM}} &= 89.0451 - 22.0417 T, T_{2,2}^{\text{MM}} = 11.0208, T_{3,0}^{\text{MM}} = -624.885 - 495.626 T + 333.353 T^2 - 28.1644 T^3, \\
T_{3,1}^{\text{MM}} &= 569.388 - 710.471 T + 84.4931 T^2, T_{3,2}^{\text{MM}} = 388.058 - 84.4931 T, T_{3,3}^{\text{MM}} = 28.1644, \\
T_{4,0}^{\text{MM}} &= -7041.01 + 5157.94 T + 2696.63 T^2 - 1100.39 T^3 + 67.4771 T^4, \\
T_{4,1}^{\text{MM}} &= -5111.88 - 6155.32 T + 3510.88 T^2 - 269.909 T^3, T_{4,2}^{\text{MM}} = 3626.15 - 3615.73 T + 404.863 T^2, \\
T_{4,3}^{\text{MM}} &= 1226.21 - 269.909 T, T_{4,4}^{\text{MM}} = 67.4771.
\end{aligned} \tag{3.16}$$

where MM represents the miniMOM scheme. The running of the strong coupling in the miniMOM is given by [69],

$$\alpha_{s,\text{MM}} = \alpha_s + 0.67862\alpha_s^2 + 0.91231\alpha_s^3 + 1.5961\alpha_s^4 + 3.1629\alpha_s^5 + \mathcal{O}(\alpha_s^6). \quad (3.17)$$

4 Renormalization-group-summed perturbation theory

Now, we discuss the perturbative expansion of the Higgs to gluons decay rate in the RGSPT. In the RGSPT, the FOPT expansion of the function $S[x(\mu), L(\mu)]$ is equivalent to writing the following new expansion,

$$S(x, L) = \sum_{n=0}^{\infty} x^n S_n(u), \quad (4.18)$$

where $u = xL$, and the function $S_n(u)$ is defined by,

$$S_n(u) \equiv \sum_{k=n}^{\infty} T_{k,k-n} u^{k-n}. \quad (4.19)$$

The main feature of the RGSPT is the explicit all-orders summations of all RG-accessible logarithms in the functions $S_n(u)$ [38, 39]. Moreover, the functions $S_n(u)$ can be derived in a closed analytical form [38, 39].

We present a derivation of the functions $S_n(u)$ in a closed analytical form using the RG invariance. The decay width of the $H \rightarrow gg$ decay defined in equation 3.10 is scale independent order-by-order in perturbation theory, and satisfies the RG equation,

$$\mu^2 \frac{d}{d\mu^2} \{ \Gamma_{H \rightarrow gg} \} = 0. \quad (4.20)$$

The above equation can be written in the following form:

$$\left[(1 - 2\gamma_m(x)) \frac{\partial}{\partial L} + \beta(x) \frac{\partial}{\partial x} + \frac{2\beta(x)}{x} \right] S(x, L) = 0, \quad (4.21)$$

where the $\overline{\text{MS}}$ β - and γ_m -functions are,

$$\begin{aligned} \beta(x) &= \mu^2 \frac{d}{d\mu^2} x(\mu) = - \left(\beta_0 x^2 + \beta_1 x^3 + \beta_2 x^4 + \dots \right), \\ \mu^2 \frac{dm}{d\mu^2} &= m \gamma_m(x(\mu)) = -m(\gamma_0 x + \gamma_1 x^2 + \gamma_2 x^3 + \dots). \end{aligned} \quad (4.22)$$

The coefficients of 5-loop QCD β -function in the $\overline{\text{MS}}$ scheme read [14],

$$\begin{aligned} \beta_0 &= 2.75 - 0.166667 n_f, \\ \beta_1 &= 6.375 - 0.791667 n_f, \\ \beta_2 &= 22.3203 - 4.36892 n_f + 0.0940394 n_f^2, \\ \beta_3 &= 114.23 - 27.1339 n_f + 1.58238 n_f^2 + 0.0058567 n_f^3, \\ \beta_4 &= 524.558 - 181.799 n_f + 17.156 n_f^2 - 0.225857 n_f^3 - 0.00179929 n_f^4, \end{aligned} \quad (4.23)$$

and the coefficients of the γ_m -function are given as [70],

$$\begin{aligned} \gamma_0 &= 1, \\ \gamma_1 &= 4.20833 - 0.138889 n_f, \\ \gamma_2 &= 19.5156 - 2.28412 n_f - 0.0270062 n_f^2, \\ \gamma_3 &= 98.9434 - 19.1075 n_f + 0.276163 n_f^2 + 0.00579322 n_f^3, \end{aligned}$$

$$\gamma_4 = 559.707 - 143.686 n_f + 7.48238 n_f^2 + 0.108318 n_f^3 - 0.0000853589 n_f^4. \quad (4.24)$$

By substituting the expansion in equation 4.18 into the equation 4.21, we write the following equation,

$$0 = (1 - 2\gamma_m(x)) \sum_{n=0}^{\infty} \sum_{k=0}^n k T_{n,k} x^n L^{k-1} + \beta(x) \sum_{n=0}^{\infty} \sum_{k=0}^n n T_{n,k} x^{n-1} L^k + \frac{2\beta(x)}{x} \sum_{n=0}^{\infty} \sum_{k=0}^n T_{n,k} x^n L^k.$$

The following recursion formula is derived by extracting the aggregate coefficient of $x^n L^{n-p}$ for $n \geq p$:

$$0 = (n - p + 1) T_{n, n-p+1} - \sum_{\ell=0}^{p-1} (n - \ell + 1) \beta_{\ell} T_{n-\ell-1, n-p} + 2 \sum_{\ell=1}^{p-1} (n - p + 1) \gamma_{\ell-1} T_{n-\ell, n-p+1}. \quad (4.25)$$

After this, we multiply both sides of equation (4.25) by u^{n-p} and sum from $n = p$ to ∞ . This results in a set of first-order linear differential equations for the functions defined in equation (4.19),

$$0 = (1 - \beta_0 u) \frac{dS_{p-1}}{du} - u \sum_{\ell=0}^{p-2} \beta_{\ell+1} \frac{dS_{p-\ell-2}}{du} + 2 \sum_{\ell=0}^{p-2} \gamma_{\ell} \frac{dS_{p-\ell-2}}{du} - \sum_{\ell=0}^{p-1} (p - \ell + 1) \beta_{\ell} S_{p-\ell-1}. \quad (4.26)$$

By substituting $n = p - 1$, the above equation can be written as,

$$(1 - \beta_0 u) \frac{dS_n}{du} - u \sum_{\ell=0}^{n-1} \beta_{\ell+1} \frac{dS_{n-\ell-1}}{du} + 2 \sum_{\ell=0}^{n-1} \gamma_{\ell} \frac{dS_{n-\ell-1}}{du} - \sum_{\ell=0}^n (n - \ell + 2) \beta_{\ell} S_{n-\ell} = 0, \quad (4.27)$$

where $n, \ell \geq 0$ with the boundary condition $S_n(0) = T_{n,0}$.

We can now solve the system of equations (4.27) iteratively in an analytical closed-form. The solutions for $n = 0, 1, 2, 3$ are,

$$\begin{aligned} S_0(u) &= \frac{T_{00}}{w_1^2}, \\ S_1(u) &= \frac{1}{\beta_0 w_1^3} \left[-2T_{00}(\beta_1 - 2\beta_0\gamma_0) \log w_1 + \beta_0 T_{00} \right], \\ S_2(u) &= \frac{1}{\beta_0^2 w_1^4} \left[\beta_0 \left(-4\beta_0^2 \gamma_1 T_{00} u + \beta_0 (2T_{00} u (2\beta_1 \gamma_0 + \beta_2) + T_{20}) - 2\beta_1^2 T_{00} u \right) - (\beta_1 - 2\beta_0\gamma_0) \log w_1 \right. \\ &\quad \left. (-4\beta_0\gamma_0 T_{00} + 3\beta_0 T_{00} + 2\beta_1 T_{00}) + 3T_{00}(\beta_1 - 2\beta_0\gamma_0)^2 \log^2 w_1 \right], \\ S_3(u) &= \frac{1}{\beta_0^3 w_1^5} \left[-\beta_0^2 \left(-2\beta_0^3 \gamma_2 T_{00} u^2 + \beta_0^2 u (2\beta_1 \gamma_1 T_{00} u + 2\beta_2 \gamma_0 T_{00} u + \beta_3 T_{00} u - 8\gamma_0 \gamma_1 T_{00} + 6\gamma_1 T_{20} + 4\gamma_2 T_{00}) \right) \right. \\ &\quad \left. - \beta_0 \left(u \left(2\beta_1^2 \gamma_0 T_{00} u + 2\beta_1 \beta_2 T_{00} u - 8\beta_1 \gamma_0^2 T_{00} + 6\beta_1 \gamma_0 T_{20} + 3\beta_2 T_{20} + 2\beta_3 T_{00} \right) + T_{30} \right) \right. \\ &\quad \left. + \beta_1 u (\beta_1 (\beta_1 T_{00} u - 4\gamma_0 T_{00} + 3T_{20}) + 2\beta_2 T_{00}) - \beta_0 (\beta_1 - 2\beta_0\gamma_0) \log w_1 \left(4\beta_1 \gamma_0 T_{00} (1 - 3\beta_0 u) \right) \right. \\ &\quad \left. - 2\beta_2 (3\beta_0 T_{00} u + T_{00}) + 2\beta_0 \left(6\beta_0 \gamma_1 T_{00} u - 4\gamma_0^2 T_{00} + 3\gamma_0 T_{20} + 2\gamma_1 T_{00} - 2T_{20} \right) + 6\beta_1^2 T_{00} u - 3\beta_1 T_{20} \right) \\ &\quad \left. - (\beta_1 - 2\beta_0\gamma_0)^2 \log^2 w_1 (-14\beta_0 \gamma_0 T_{00} + 6\beta_0 T_{20} + 7\beta_1 T_{00}) + 4T_{00} (\beta_1 - 2\beta_0\gamma_0)^3 \log^3 w_1 \right], \quad (4.28) \end{aligned}$$

where $w_1 = 1 - \beta_0 u$.

The new RGS expansions now can be written as,

$$\begin{aligned} S_{RGSPT}^{NLO} &= S_0(xL) + xS_1(xL), \\ S_{RGSPT}^{N^2LO} &= S_0(xL) + xS_1(xL) + x^2S_2(xL), \\ S_{RGSPT}^{N^3LO} &= S_0(xL) + xS_1(xL) + x^2S_2(xL) + x^3S_3(xL), \end{aligned} \quad (4.29)$$

$$S_{RGSP T}^{N^4LO} = S_0(xL) + xS_1(xL) + x^2S_2(xL) + x^3S_3(xL) + x^4S_4(xL).$$

In the SI, OS, and miniMOM schemes, mass appearing in the logarithms does not depend on the RG scale μ . Therefore, the closed-form analytic expressions of the functions $S_n(u)$ in these schemes are obtained by solving equation 4.27 after substituting the coefficient of the anomalous γ functions γ_i to be zero.

5 Scale and scheme dependence in the FOPT

We now investigate the perturbative behaviour of the Higgs to gluons decay width by studying the scale dependence in the FOPT in the \overline{MS} , SI, OS, and miniMOM schemes. Our numerical inputs are given in table 1. Moreover, for running the strong coupling and quark masses, we use the Mathematica package ‘‘RunDec’’ [71].

Parameter	Value
M_H	125.25 ± 0.17 [72]
G_F	1.1663787×10^{-5} GeV [72]
$\alpha_s[M_Z]$	0.1179 ± 0.0009 [72]
$M_{t_{OS}}$	173 GeV [72]
$M_{t_{SI}}$	164 GeV [72]

Table 1: The numerical values of masses and couplings used in this work.

The Higgs to gluons decay width is normalized by the first term in the expansion, i.e. Γ_0 given by,

$$\Gamma_0 = G_F M_H^3 / (36\pi^3 \sqrt{2}) (\alpha_s(M_H^2))^2 = 0.00018378, \quad (5.30)$$

where $\alpha_s(M_H^2) = 0.112602$ is calculated using the Mathematica package ‘‘RunDec’’ [71]. We use the above value of Γ_0 in all our predictions.

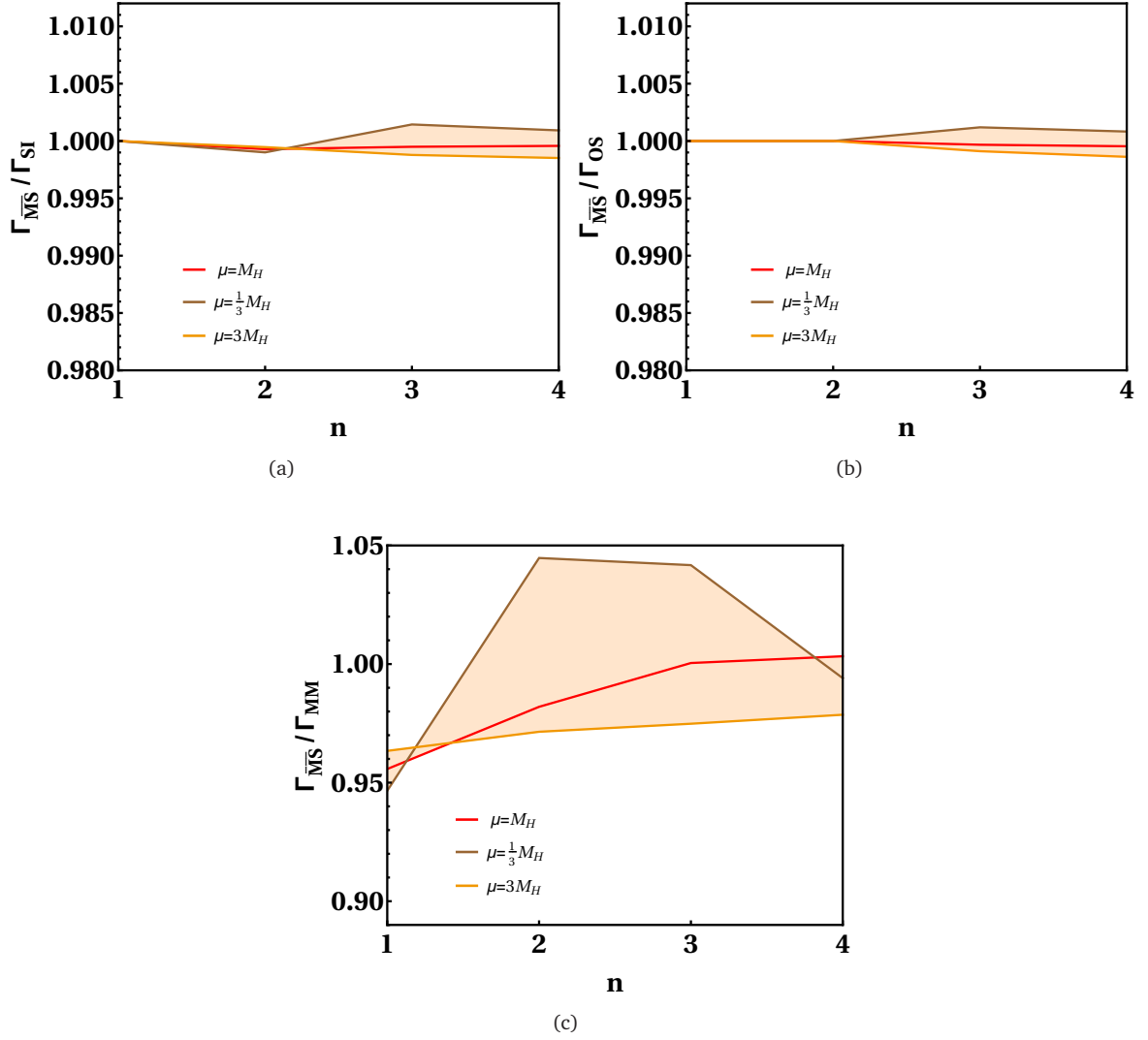


Figure 1: The variation of $\Gamma_{\overline{\text{MS}}}/\Gamma_{\text{scheme}}$ at RG scales $\mu = \frac{1}{3}M_H, M_H,$ and $3M_H$ in the FOPT in the (a)SI (b)OS and (c)miniMOM schemes up to order $n = 4$.

We show the RG scale dependence of the ratio of the Higgs to gluons decay width in two different RG schemes in the FOPT in figure 1. To compare the predictions of different RG schemes, we have chosen the $\overline{\text{MS}}$ scheme as the reference scheme. The behaviour of the OS scheme is closer to that of the $\overline{\text{MS}}$ scheme due the same mass of the top quark used in both schemes.

In the $\overline{\text{MS}}$ scheme, the contribution of the N^4LO correction (defined by $\Gamma_{\text{N}^4\text{LO}} \times 100/\Gamma$) to the $\Gamma(H \rightarrow gg)$ decay width at the renormalization scale $\mu = M_H$ for the on shell top quark mass is -0.6% . We now vary the scale for a range of $\mu = \frac{1}{3}M_H$ to $\mu = 3M_H$, and find that the contribution of the N^4LO corrections to the $\Gamma(H \rightarrow gg)$ in the $\overline{\text{MS}}$ scheme is 0.2% and 2% , respectively. The decay width in this range is $\Gamma(H \rightarrow gg) = 1.836\Gamma_0$ at the RG scale $\mu = \frac{1}{3}M_H$, $\Gamma(H \rightarrow gg) = 1.842\Gamma_0$ at the RG scale $\mu = M_H$, and $\Gamma(H \rightarrow gg) = 1.838\Gamma_0$ at the RG scale $\mu = 3M_H$. The N^4LO contribution in the SI and OS schemes is approximately identical to that of the $\overline{\text{MS}}$ scheme. The decay width in this range is $\Gamma(H \rightarrow gg) = 1.834\Gamma_0$ at the RG scale $\mu = \frac{1}{3}M_H$, $\Gamma(H \rightarrow gg) = 1.843\Gamma_0$ at the RG scale $\mu = M_H$, and $\Gamma(H \rightarrow gg) = 1.841\Gamma_0$ at the RG scale $\mu = 3M_H$ in the SI and OS schemes.

On the other hand, the N^4LO contribution in the miniMOM scheme is -1.06% at RG scale $\mu = M_H$. At

RG scale $\mu = M_H/3$, the N⁴LO correction in the miniMOM scheme is 5.55% which is quite large. The N⁴LO contribution at RG scale $\mu = 3M_H$ is 0.68%. The decay width in this range is $\Gamma(H \rightarrow gg) = 1.847\Gamma_0$ at the RG scale $\mu = \frac{1}{3}M_H$, $\Gamma(H \rightarrow gg) = 1.836\Gamma_0$ at the RG scale $\mu = M_H$, and $\Gamma(H \rightarrow gg) = 1.879\Gamma_0$ at the RG scale $\mu = 3M_H$ in this scheme. We observe that the miniMOM scheme is quite sensitive to the scale variation, and relatively away from the predictions of the $\overline{\text{MS}}$ scheme.

6 Scale and scheme dependence in the RGSPT

In this section, we discuss the behaviour of the RGSPT expansions of the Higgs to gluons decay width in the $\overline{\text{MS}}$, SI, OS, and miniMOM schemes. The variation of the ratio of the Higgs to gluons decay width in two different RG schemes at different orders is shown in figure 2. There is a relatively small difference between the FOPT and RGSPT predictions of the $\Gamma_{\overline{\text{MS}}}/\Gamma_{\text{SI}}$ upto order $n = 3$ due to the different numerical values of the top-quark mass used in these schemes.

We begin our discussion by studying the behaviour of the RGSPT expansions in the $\overline{\text{MS}}$ scheme at the RG scale $\mu = M_H$ using the on shell top quark mass. The contribution of the N⁴LO correction to the $\Gamma(H \rightarrow gg)$ decay width at the RG scale $\mu = M_H$ is found to be -0.06% in the $\overline{\text{MS}}$ scheme. At the RG scale $\mu = \frac{1}{3}M_H$, this contribution becomes -0.18% and changes to 0.04% at the RG scale $\mu = 3M_H$. The decay width at the RG scales $\mu = \frac{1}{3}M_H$, $\mu = M_H$, and $\mu = 3M_H$ is $\Gamma(H \rightarrow gg) = 1.845\Gamma_0$. This actually shows that the RGSPT expansion is considerably less sensitive to the RG scale μ . We observe that at the RG scale $\mu = M_H$, the N⁴LO correction in the SI and OS schemes is -0.16% and -0.03% , respectively. This correction becomes -0.28% in the SI scheme and -0.15% in the OS scheme at the RG scale $\mu = \frac{1}{3}M_H$, and is -0.06% and 0.07% , respectively, at the RG scale $\mu = 3M_H$.

Now we turn our attention towards the miniMOM scheme, and discuss our results in this scheme for the RGSPT expansions. We have already observed that in the FOPT, this scheme is relatively more sensitive to the RG scale μ . The N⁴LO contribution in this scheme at $\mu = M_H$ is -1.01% , which is large as compared to other used schemes. The N⁴LO contribution at RG scales $\mu = \frac{1}{3}M_H$ and $\mu = 3M_H$ is -1.05% and -0.96% respectively. The important observation is that this N⁴LO contribution remains stable relative to the RG scale in the RGSPT expansion even at $\mu = \frac{1}{3}M_H$ and $\mu = 3M_H$. The decay width in this range is $\Gamma(H \rightarrow gg) = 1.855\Gamma_0$ at the RG scale $\mu = \frac{1}{3}M_H$, $\Gamma(H \rightarrow gg) = 1.853\Gamma_0$ at the RG scale $\mu = M_H$, and $\Gamma(H \rightarrow gg) = 1.851\Gamma_0$ at the RG scale $\mu = 3M_H$ in this scheme.

7 Asymptotic Padé approximant improved $H \rightarrow gg$ decay rate

The Padé approximant is a nonlinear method of summing series that can be considered as an approximate analytic continuation [73]. It is widely applied to determine higher-order terms in a number of field-theoretical perturbative expansions, including β - and γ -functions of QCD at four- and five-loops [56, 57, 58, 59, 60, 61, 62, 63, 64].

We begin by considering a generic perturbative expansion of the form,

$$S \equiv 1 + R_1x + R_2x^2 + R_3x^3 + R_4x^4 + \dots, \quad (7.31)$$

where the coefficients $\{R_1, R_2, R_3, R_4\}$ are known and the coefficients $\{R_5, \dots\}$ are unknown.

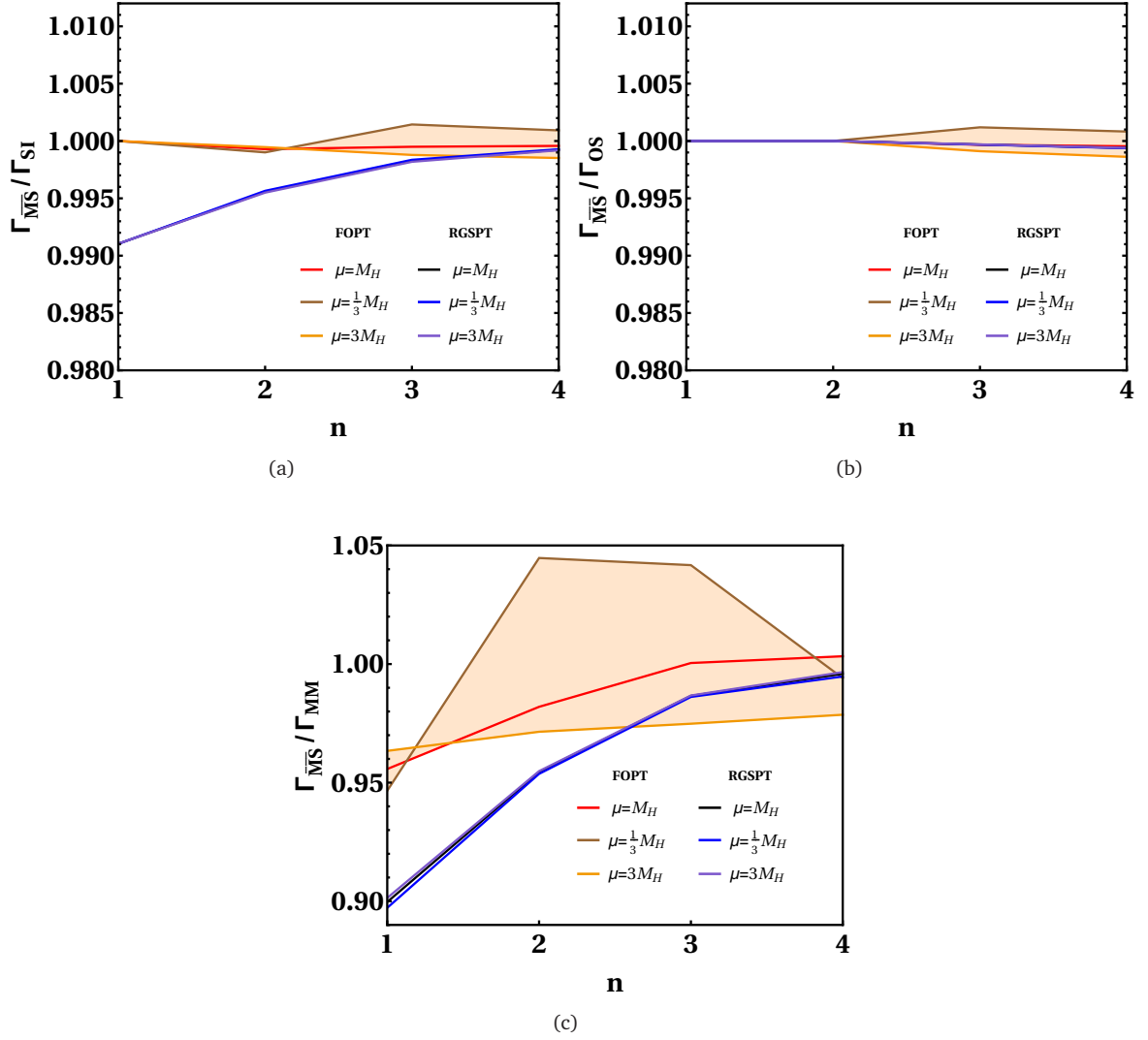


Figure 2: The variation of $\Gamma_{\overline{MS}}/\Gamma_{\text{scheme}}$ at RG scales $\mu = \frac{1}{3}M_H, M_H,$ and $3M_H$ in the FOPT and RGSPT in the (a)SI (b)OS and (c)miniMOM schemes up to order $n = 4$.

The Padé approximant to a generic perturbative expansion is denoted by,

$$\begin{aligned}
 S_{[N|M]} &\equiv \frac{1 + a_1x + a_2x^2 + \dots + a_Nx^N}{1 + b_1x + b_2x^2 + \dots + b_Mx^M} \\
 &= 1 + R_1x + R_2x^2 + R_3x^3 + R_4x^4 + \dots + R_{N+M+1}x^{N+M+1} + \dots
 \end{aligned} \tag{7.32}$$

The asymptotic error in the Padé approximant prediction is given by[59],

$$\delta_{N+M+1} = \frac{R_{N+M+1}^{\text{Padé}} - R_{N+M+1}}{R_{N+M+1}} = -\frac{M!A^M}{[N + M + aM + b]^M} = \delta_i, \tag{7.33}$$

where $R_{N+M+1}^{\text{Padé}}$ is the $[N|M]$ Padé approximant prediction and R_{N+M+1} is the exact value of this coefficient. The free parameters $\{A, a, b\}$ are chosen to produce the best results [59]. In this section, we choose $a = -b = 10^6$ which provide the best predictions. Moreover, for such large values of a and b , the error δ_i becomes very small.

If the coefficient R_1 is known, we can choose $N = 0$ and $M = 1$ and write the $[0|1]$ Padé approximant as,

$$S_{[0|1]} = \frac{1}{1 + b_1 x} = 1 - b_1 x + b_1^2 x^2 + \dots = 1 + R_1 x + R_2^{Padé} x^2 + \dots, \quad (7.34)$$

where $R_2^{Padé} = R_1^2$ is the Padé approximant prediction for the next unknown higher-order term in the generic perturbative series in equation 7.31.

The asymptotic error formula in equation 7.33 provides the following equation for the $[0|1]$ Padé approximant,

$$\frac{R_2^{Padé} - R_2}{R_2} = \frac{R_1^2 - R_2}{R_2} = \frac{-A}{1 + (a + b)}, \quad (7.35)$$

which gives the value of A as,

$$A = (1 + a + b) \left(1 - \frac{R_1^2}{R_2} \right). \quad (7.36)$$

We can determine the $[2|2]$ Padé approximant given the knowledge of only R_1, R_2, R_3 and R_4 . It is given by,

$$\begin{aligned} S_{[2|2]} = \frac{1 + a_1 x + a_2 x}{1 + b_1 x + b_2 x} &= 1 + (a_1 - b_1) x + (a_2 - a_1 b_1 + b_1^2 - b_2) x^2 \\ &+ (-a_2 b_1 - b_1^3 + a_1(b_1^2 - b_2) + 2b_1 b_2) x^3 \\ &+ (-a_1 b_1^3 + b_1^4 + a_2(b_1^2 - b_2) + 2a_1 b_1 b_2 - 3b_1^2 b_2 + b_2^2) x^4 \\ &+ (-b_1^5 + 4b_1^3 b_2 - 3b_1 b_2^2 - a_2(b_1^3 - 2b_1 b_2) + a_1(b_1^4 - 3b_1^2 b_2 + b_2^2)) x^5 + \dots \\ &= 1 + R_1 x + R_2 x^2 + R_3 x^3 + R_4 x^4 + R_5^{Padé} x^5 + \dots. \end{aligned} \quad (7.37)$$

The $[2|2]$ Padé approximant predicts,

$$R_5^{Padé} = \frac{R_3^3 - 2R_2 R_3 R_4 + R_1 R_4^2}{-R_2^2 + R_1 R_3}. \quad (7.38)$$

The asymptotic error can be written as,

$$\frac{R_5^{Padé} - R_5}{R_5} = \frac{-2A^2}{(4 + 2a + b)^2} \equiv \delta_5. \quad (7.39)$$

This error allows us to estimate an improved value of the true value R_5 , which is referred to as asymptotic Padé approximant prediction (APAP) in literature [59]. Thus, our APAP estimate of the true value R_5 is,

$$\begin{aligned} R_5 &= \frac{(-R_3^3 + 2R_2 R_3 R_4 - R_1 R_4^2)}{(1 + \delta_5)(R_2^2 - R_1 R_3)} \\ &= \frac{8R_2^2(R_3^3 - 2R_2 R_3 R_4 + R_1 R_4^2)}{(R_1^4 - 2R_1^2 R_2 - 7R_2^2)(R_2^2 - R_1 R_3)}. \end{aligned} \quad (7.40)$$

Now, we apply the APAP formalism to predict N⁵LO term of the $\Gamma(H \rightarrow gg)$ decay width in the FOPT. For the sake of clarity and reliability, we present our analysis in the $\overline{\text{MS}}$, SI, OS and miniMOM schemes. The $\Gamma(H \rightarrow gg)$ decay width is given in equation 3.10 where the perturbative expansion $S[x(\mu), L(\mu)]$ now can be written as,

$$S_{\text{FOPT}}[x(\mu), L(\mu)] = \sum_{n=0}^{\infty} \sum_{k=0}^n T_{n,k} x^n L^k = \sum_{n=0}^{\infty} R_n x^n, \quad (7.41)$$

where

$$R_n[L(\mu)] = \sum_{k=0}^n T_{n,k} L^k. \quad (7.42)$$

such that

$$R_5[L] = T_{5,0} + T_{5,1}L + T_{5,2}L^2 + T_{5,3}L^3 + T_{5,4}L^4 + T_{5,5}L^5, \quad (7.43)$$

where $T_{5,0}, T_{5,1}, T_{5,2}, T_{5,3}, T_{5,4}$ and $T_{5,5}$ are the unknown higher-order coefficients. The coefficients $T_{5,1} - T_{5,5}$ can be predicted with the help of the RG invariance of $\Gamma(H \rightarrow gg)$ decay width. The coefficient $T_{5,0}$ is not available through the RG invariance.

Thus, we use equation 4.21 obtained from the RG invariance of $\Gamma(H \rightarrow gg)$ decay width to predict the coefficients $T_{5,1} - T_{5,5}$. This means that the perturbative validity of equation 4.21 to order $x^5 L^5$ can determine the six-loop coefficients provided the x^5 contribution of equation 4.21 vanishes. Thus, in the $\overline{\text{MS}}$ scheme we obtain,

$$\begin{aligned} T_{5,1}^{\overline{\text{MS}}} &= -0.251403n_f^5 + 52.4477n_f^4 - 2974.99n_f^3 + 64964.7n_f^2 - 569877.n_f + 1.58072 \times 10^6, \\ T_{5,2}^{\overline{\text{MS}}} &= 2.23573n_f^4 - 306.398n_f^3 + 11315.1n_f^2 - 148924.n_f + 600692, \\ T_{5,3}^{\overline{\text{MS}}} &= -0.0357832n_f^4 - 7.47604n_f^3 + 752.153n_f^2 - 16703.8n_f + 104439, \\ T_{5,4}^{\overline{\text{MS}}} &= -0.00462963n_f^4 + 0.319155n_f^3 + 12.6003n_f^2 - 784.131n_f + 8181.75, \\ T_{5,5}^{\overline{\text{MS}}} &= 222.674 - 13.4954n_f. \end{aligned} \quad (7.44)$$

In the SI scheme, the coefficients are as follows,

$$\begin{aligned} T_{5,1}^{\text{SI}} &= -0.251403n_f^5 + 51.897n_f^4 - 2904.65n_f^3 + 62487.4n_f^2 - 538466n_f + 1.45824 \times 10^6, \\ T_{5,2}^{\text{SI}} &= 2.23573n_f^4 - 302.321n_f^3 + 11022.4n_f^2 - 143316.n_f + 569814, \\ T_{5,3}^{\text{SI}} &= -0.0357832n_f^4 - 7.30602n_f^3 + 737.153n_f^2 - 16307.8n_f + 101326, \\ T_{5,4}^{\text{SI}} &= -0.00462963n_f^4 + 0.319155n_f^3 + 12.6003n_f^2 - 776.921n_f + 8062.79, \\ T_{5,5}^{\text{SI}} &= 222.674 - 13.4954n_f. \end{aligned} \quad (7.45)$$

The coefficients obtained in the OS scheme are,

$$\begin{aligned} T_{5,1}^{\text{OS}} &= -0.251403n_f^5 + 52.4682n_f^4 - 2966.69n_f^3 + 64629.9n_f^2 - 566720.n_f + 1.57759 \times 10^6, \\ T_{5,2}^{\text{OS}} &= 2.23573n_f^4 - 305.229n_f^3 + 11256.9n_f^2 - 148434.n_f + 602130, \\ T_{5,3}^{\text{OS}} &= -0.0357832n_f^4 - 7.29085n_f^3 + 744.961n_f^2 - 16652.6n_f + 104721, \\ T_{5,4}^{\text{OS}} &= -0.00462963n_f^4 + 0.319155n_f^3 + 12.6003n_f^2 - 784.131n_f + 8181.75, \\ T_{5,5}^{\text{OS}} &= 222.674 - 13.4954n_f, \end{aligned} \quad (7.46)$$

whereas the coefficients obtained in the miniMOM scheme are,

$$\begin{aligned} T_{5,1}^{\text{MM}} &= -0.00359858n_f^4 - 0.168327n_f^3 + 150.512n_f^2 + 6047.03n_f - 136552, \\ T_{5,2}^{\text{MM}} &= 0.033676n_f^3 + 28.524n_f^2 - 3364.45n_f + 25534.1, \\ T_{5,3}^{\text{MM}} &= 1.38186n_f^2 - 2691.8n_f + 38749.9, \\ T_{5,4}^{\text{MM}} &= 6001.76 - 378.012n_f, \\ T_{5,5}^{\text{MM}} &= 222.675 - 13.4954n_f. \end{aligned} \quad (7.47)$$

Now, we use the APAP method to predict the six-loop coefficients $\{T_{5,0} - T_{5,5}\}$ in the $\overline{\text{MS}}$, SI, OS, and miniMOM schemes. The reliability of these APAP predicted coefficients will be estimated by calculating the uncertainty in their predictions against the RGE predicted $\{T_{5,1} - T_{5,5}\}$ coefficients. For this purpose, we define

the moments of $R_5(w)$, where $w = m_t^2(\mu)/\mu^2$; ($L = -\ln(w)$), over the perturbative region $0 < w \leq 1$ in the following manner,

$$N_k \equiv (k+2) \int_0^1 dw w^{k+1} R_5(w). \quad (7.48)$$

We substitute equation 7.43 into equation 7.48, which results in a set of equations for moments given by,

$$\begin{aligned} N_{-1} &= T_{5,0} + T_{5,1} + 2(T_{5,2} + 3T_{5,3} + 12T_{5,4} + 60T_{5,5}), \\ N_0 &= \frac{1}{4}(4T_{5,0} + 2T_{5,1} + 2T_{5,2} + 3T_{5,3} + 6T_{5,4} + 15T_{5,5}), \\ N_1 &= \frac{1}{81}(81T_{5,0} + 27T_{5,1} + 18T_{5,2} + 18T_{5,3} + 24T_{5,4} + 40T_{5,5}), \\ N_2 &= \frac{1}{128}(128T_{5,0} + 32T_{5,1} + 16T_{5,2} + 12T_{5,3} + 12T_{5,4} + 15T_{5,5}), \\ N_3 &= \frac{1}{625}(625T_{5,0} + 125T_{5,1} + 50T_{5,2} + 30T_{5,3} + 24T_{5,4} + 24T_{5,5}), \\ N_4 &= \frac{1}{324}(324T_{5,0} + 54T_{5,1} + 18T_{5,2} + 9T_{5,3} + 6T_{5,4} + 5T_{5,5}). \end{aligned} \quad (7.49)$$

The above moments can be numerically computed by substituting equation 7.40 into the integrand of equation 7.48 with $L = -\ln(w)$. The six-loop coefficients $T_{5,0}^{Pad\acute{e}} - T_{5,5}^{Pad\acute{e}}$ are determined by substituting these numerical values in equation 7.49. The APAP predictions are compared to the RGE predictions for $n_f = 5$ flavours obtained from equations 7.44-7.47. We estimate the relative error of the APAP predictions of the coefficients $T_{5,1} - T_{5,5}$ by computing $\delta T_{5,i}^{Pad\acute{e}} \equiv (T_{5,i}^{Pad\acute{e}} - T_{5,i})/T_{5,i}$. Our predictions for the $\overline{\text{MS}}$, SI, OS, and the miniMOM schemes are given in tables 2-5.

$\overline{\text{MS}}$	$T_{5,0}$	$T_{5,1}$	$T_{5,2}$	$T_{5,3}$	$T_{5,4}$	$T_{5,5}$
<i>Padé</i>	-110686	12383.7	100812	39138.2	4417.21	199.466
RGE	-	15570.1	102046	38766.7	4613.1	155.197
$\delta T_{5,i}^{Pad\acute{e}}$	-	20.5%	1.2%	1.0%	4.2%	28.5%

Table 2: The APAP predictions of the coefficients R_5 using the $S[1|3]$ Padé approximant in the $\overline{\text{MS}}$ scheme with errors.

SI	$T_{5,0}$	$T_{5,1}$	$T_{5,2}$	$T_{5,3}$	$T_{5,4}$	$T_{5,5}$
<i>Padé</i>	-110378	-4477.15	92857.5	37021	4684.3	139.191
RGE	-	-3333.48	92400.3	37279.7	4530.19	155.197
$\delta T_{5,i}^{Pad\acute{e}}$	-	34.3%	0.5%	0.7%	3.4%	10.3%

Table 3: The APAP predictions of the coefficients R_5 using the $S[1|3]$ Padé approximant in the SI scheme with errors.

OS	$T_{5,0}$	$T_{5,1}$	$T_{5,2}$	$T_{5,3}$	$T_{5,4}$	$T_{5,5}$
<i>Padé</i>	-105076	19853.1	104463	39648.4	4417.98	188.272
RGE	-	20907.1	104628	39147.8	4613.1	155.197
$\delta T_{5,i}^{Padé}$	-	5.0%	0.2%	1.3%	4.2%	21.3%

Table 4: The APAP predictions of the coefficients R_5 using the $S[1|3]$ Padé approximant in the OS scheme with errors.

miniMOM	$T_{5,0}$	$T_{5,1}$	$T_{5,2}$	$T_{5,3}$	$T_{5,4}$	$T_{5,5}$
<i>Padé</i>	-72320.9	-118501	10748.5	23659	2586.12	197.956
RGE	-	-102578	9429.12	25325.4	4111.7	155.197
$\delta T_{5,i}^{Padé}$	-	15.5%	14%	6.6%	37%	27.6%

Table 5: The APAP predictions of the coefficients R_5 using the $S[2|2]$ Padé approximant in the miniMOM scheme with errors.

We observe that there is a good agreement between the APAP and RGE predictions of the $T_{5,1} - T_{5,5}$ coefficients in all the four schemes. This gives us the required confidence in the APAP predictions of these coefficients, and suggests the credibility of the APAP prediction of the coefficient $T_{5,0}$ which is inaccessible through the RG-invariance.

The predictions of the coefficients R_i for $i = 5 - 9$ of the perturbative expansions in the \overline{MS} , SI, OS, and miniMOM schemes are given in table 6, where the coefficients for $i = 6 - 9$ are computed using the $[3|2]$, $[4|2]$, $[5|2]$, $[6|2]$ Padé approximants. We compare these predictions to that predicted by RGE in the third column. The coefficient $T_{5,0}$ is not accessible through the RGE predictions. Therefore, for the prediction of the coefficient R_5^{RGE} , we assume the $T_{5,0}$ of the RGE identical to the $T_{5,0}$ of the Padé prediction.

Scheme	$R_5^{Padé}$	R_5^{RGE}	$\delta R_5^{Padé}$	$R_6^{Padé}$	$R_7^{Padé}$	$R_8^{Padé}$	$R_9^{Padé}$
\overline{MS}	-86422.1	-87826.6	1.6 %	-285341	3.3315×10^6	4.83632×10^7	1.99309×10^8
SI	-86387.5	-87191.2	0.9 %	-266735	3.53838×10^6	4.82802×10^7	1.75429×10^8
OS	-84249.7	-84689.2	0.5 %	-280858	3.14976×10^6	4.5776×10^7	1.87582×10^8
miniMOM	2761.63	-8253.07	133%	496045	2.82424×10^6	-1.66589×10^7	-2.93284×10^8

Table 6: The APAP predicted values of R_{5-9} at $\mu = M_H$ and RGE predicted value of R_5 at $\mu = M_H$ with their relative error $\delta R_5^{Padé}$, where $\delta R_5^{Padé} = (R_5^{RGE} - R_5^{Padé})/R_5^{RGE} \times 100$ in the \overline{MS} , SI, OS, and miniMOM schemes.

We notice from table 6 that the overall coefficient R_5 is negative in the \overline{MS} , SI, and OS schemes, and is in an agreement with that predicted from the use of RGE. This can be seen in the fourth column where the uncertainty $\delta R_5^{Padé}$ between the Padé and RGE predictions is computed. The largest uncertainty is 1.6 % in the \overline{MS} scheme. However, the coefficient R_5 is positive in the miniMOM scheme, and the uncertainty is quite large. Therefore, the miniMOM scheme is not working well in the APAP formalism, and its predictions are not reliable. This particular feature of the miniMOM scheme continues to hold in the PBA formalism as well.

The asymptotic errors δ_i , defined in equation 7.33, on our predictions presented in 6 are computed in the four different schemes, and given in table 7.

Scheme	δ_5	δ_6	δ_7	δ_8	δ_9
$\overline{\text{MS}}$	9.89×10^{-19}	-2.40×10^{-12}	-2.40×10^{-12}	-2.40×10^{-12}	-2.40×10^{-12}
SI	9.66×10^{-19}	-2.66×10^{-12}	-2.37×10^{-12}	-2.37×10^{-12}	-2.37×10^{-12}
OS	-9.89×10^{-19}	-2.40×10^{-12}	-2.40×10^{-12}	-2.40×10^{-12}	-2.40×10^{-12}
miniMOM	-2.19×10^{-11}				

Table 7: Asymptotic errors for R_{5-9} in the $\overline{\text{MS}}$, SI, OS, and miniMOM schemes.

The prediction of the coefficients $T_{4,i}$ and their relative errors $\delta T_{4,i}^{\text{Padé}} \equiv (T_{4,i}^{\text{Padé}} - T_{4,i})/T_{4,i} \times 100$ are obtained using the [0|3] Padé approximant. These predictions in the $\overline{\text{MS}}$, SI, OS, and miniMOM schemes are given in tables 8-11.

$\overline{\text{MS}}$	$T_{4,0}$	$T_{4,1}$	$T_{4,2}$	$T_{4,3}$	$T_{4,4}$
<i>Padé</i>	-1543.32	14291.6	9654.97	1577.93	67.477
Known	-453.772	15627.2	9595.85	1574.97	67.4771
$\delta T_{4,i}^{\text{Padé}}$	240.1%	8.5%	0.6%	0.2%	0.0002%

Table 8: The APAP predictions of the coefficients R_4 in the $\overline{\text{MS}}$ scheme with errors.

SI	$T_{4,0}$	$T_{4,1}$	$T_{4,2}$	$T_{4,3}$	$T_{4,4}$
<i>Padé</i>	-2911.26	12890.6	9263.72	1549.09	67.4769
Known	-1891.18	14042.3	9217.44	1546.13	67.4771
$\delta T_{4,i}^{\text{Padé}}$	53.9%	8.2%	0.5%	0.2%	0.0003%

Table 9: The APAP predictions of the coefficients R_4 in the SI scheme with errors.

OS	$T_{4,0}$	$T_{4,1}$	$T_{4,2}$	$T_{4,3}$	$T_{4,4}$
<i>Padé</i>	-922.469	14873.9	9742.49	1577.93	67.477
Known	-5.68386	16064.3	9695.27	1574.97	67.4771
$\delta T_{4,i}^{\text{Padé}}$	16129%	7.4%	0.5%	0.2%	0.0001%

Table 10: The APAP predictions of the coefficients R_4 in the OS scheme with errors.

miniMOM	$T_{4,0}$	$T_{4,1}$	$T_{4,2}$	$T_{4,3}$	$T_{4,4}$
<i>Padé</i>	-8551.44	-493.732	6798.1	1571.28	67.4771
Known	-8939.29	401.918	6130.7	1400.56	67.4771
$\delta T_{4,i}^{Padé}$	4.3%	222.8%	10.9%	12.2%	0.00004%

Table 11: The APAP predictions of the coefficients R_4 in the miniMOM scheme with errors.

We note that the APAP formalism in this case is not able to reproduce the leading coefficient $T_{4,0}$ in the \overline{MS} , SI, and OS schemes. In the case of the miniMOM scheme, this happens with the coefficient $T_{4,1}$. However, we also notice that the overall coefficient R_4 of the perturbative expansion is in a good agreement with the APAP predictions as shown in table 12. Moreover, we shall show in the next section that the asymptotic Padé-Borel approximant is capable of improving the APAP predictions of the coefficients $T_{4,i}$, therefore reproducing the known coefficient R_4 with a better accuracy.

Scheme	R_4	$R_4^{Padé}$	δR_4	δ_4
\overline{MS}	-6957.06	-7159.99	2.9 %	9.88566×10^{-19}
SI	-7019.12	-7405.32	5.5%	9.66238×10^{-19}
OS	-6749.84	-6878.79	1.9%	9.88566×10^{-19}
miniMOM	-7006.54	-5807.67	17.1%	2.72026×10^{-17}

Table 12: The APAP predicted values of R_4 at $\mu = M_H$ with relative error δR_4 and asymptotic error δ_4 , where $\delta R_4 = (R_4 - R_4^{Padé})/R_4 \times 100$.

We observe that the accuracy obtained in the predictions of the six-loop coefficients $T_{5,1}^{Padé} - T_{5,5}^{Padé}$ using the APAP method, in particular for the \overline{MS} and OS schemes imply that we can employ the APAP formalism with confidence elsewhere. Therefore, we now use the APAP algorithm to predict the coefficients $\beta_5 - \beta_9$ and $\gamma_5 - \gamma_9$, the higher-order loop corrections to the β and γ functions. These coefficients will be used to compute the RGSPT function $S_5(u) - S_9(u)$.

The β function defined in equation 4.22 can be written as,

$$\beta(x) = -\beta_0 x^2 \sum_{i=0}^{\infty} R_i x^i, \quad (7.50)$$

where $R_i \equiv \beta_i/\beta_0$. Using the already known values of β_0 to β_4 given in equation 4.23, we estimate the values of $\beta_5, \beta_6, \beta_7, \beta_8$ and β_9 for $n_f = 5$ using [1|3], [3|2], [4|2], [5|2] and [6|2] Padé approximants respectively. The values of $\beta_5 - \beta_9$ obtained are as follows,

$$\beta_5 = 54.8149, \beta_6 = 61.6663, \beta_7 = 166.748, \beta_8 = 228.033, \beta_9 = 524.048. \quad (7.51)$$

The γ_m function as defined in equation 4.22 can be written as

$$\gamma_m(x) = x \sum_{i=0}^{\infty} R_i x^i, \quad (7.52)$$

where $R_i = \gamma_i$.

We use [1|3], [3|2], [4|2], [5|2] and [6|2] Padé approximants to predict the values of $\gamma_5, \gamma_6, \gamma_7, \gamma_8$ and γ_9 respectively using the already known values of $\gamma_0 - \gamma_4$ for $n_f = 5$. The predictions for $\gamma_5 - \gamma_9$ are as follows,

$$\gamma_5 = 659.411, \gamma_6 = 14271.8, \gamma_7 = 316090, \gamma_8 = 7.01049 \times 10^6, \gamma_9 = 1.55497 \times 10^8. \quad (7.53)$$

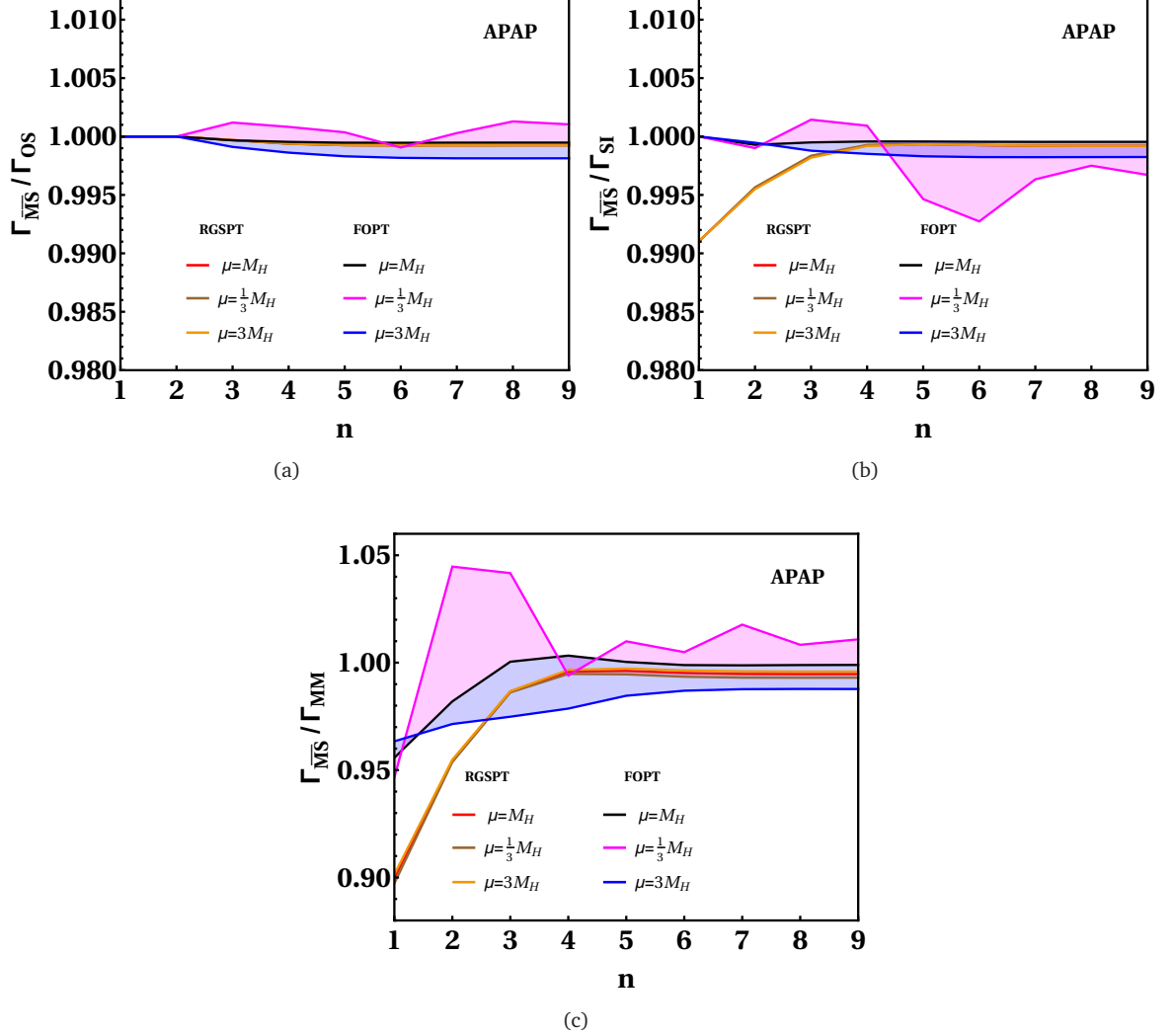


Figure 3: The variation of $\Gamma_{\overline{\text{MS}}}/\Gamma_{\text{scheme}}$ at RG scales $\mu = \frac{1}{3}M_H, M_H,$ and $3M_H$ in the FOPT and RGSPT in the (a)SI (b)OS and (c)miniMOM schemes up to order $n = 9$.

Now we discuss the implications of the APAP determination of the coefficients $T_{n,k}, \beta_n$ and γ_n ($n = 5 - 9$) to the $\Gamma(H \rightarrow gg)$ decay width in the FOPT and RGSPT. For a better understanding, we present the higher-order behaviour of the ratio of the Higgs to gluons decay width in two different RG schemes at different orders in the FOPT and RGSPT in figure 3. The $\overline{\text{MS}}$ and the OS schemes are showing very similar behaviour. The RGSPT predictions reside within the FOPT predictions in this case. In the case of the SI scheme, this occurs beyond $n = 3$. The miniMOM scheme is again not performing well. However, it becomes stable within the framework of the RGSPT beyond $n = 3$.

We provide order-by-order perturbative evaluation of the $\Gamma(H \rightarrow gg)$ decay width up to N⁵LO at $\mu = M_H$ in the FOPT using the APAP formalism as,

$$\begin{aligned}
\frac{\Gamma_{\text{Padé}}^{\overline{\text{MS}}}(M_H)}{\Gamma_{\text{LO}}(M_H)} &= 1 + 0.641657 + 0.196393 + 0.0176989 - 0.0114448 - \boxed{0.00742209}, & (7.54) \\
\frac{\Gamma_{\text{Padé}}^{\text{SI}}(M_H)}{\Gamma_{\text{LO}}(M_H)} &= 1 + 0.641657 + 0.197175 + 0.0178975 - 0.0115469 - \boxed{0.0074973}, \\
\frac{\Gamma_{\text{Padé}}^{\text{OS}}(M_H)}{\Gamma_{\text{LO}}(M_H)} &= 1 + 0.641657 + 0.196393 + 0.0180594 - 0.0111039 - \boxed{0.00716578}, \\
\frac{\Gamma_{\text{Padé}}^{\text{MM}}(M_H)}{\Gamma_{\text{LO}}(M_H)} &= 1 + 0.533291 + 0.0659834 - 0.0398094 - 0.0163109 + \boxed{0.000251122}.
\end{aligned}$$

Similar predictions of the $\Gamma(H \rightarrow gg)$ decay width up to N⁵LO at $\mu = M_H$ in RGSPT using the APAP formalism are,

$$\begin{aligned}
\frac{\Gamma_{\text{Padé}}^{\overline{\text{MS}}}(M_H)}{\Gamma_{\text{LO}}(M_H)} &= 1 + 0.695577 + 0.263334 + 0.0546671 - 0.00126852 - \boxed{0.00527992}, & (7.55) \\
\frac{\Gamma_{\text{Padé}}^{\text{SI}}(M_H)}{\Gamma_{\text{LO}}(M_H)} &= 1 + 0.686965 + 0.253127 + 0.0487537 - 0.00318015 - \boxed{0.00542712}, \\
\frac{\Gamma_{\text{Padé}}^{\text{OS}}(M_H)}{\Gamma_{\text{LO}}(M_H)} &= 1 + 0.695577 + 0.263334 + 0.055281 - 0.000655924 - \boxed{0.00502101}, \\
\frac{\Gamma_{\text{Padé}}^{\text{MM}}(M_H)}{\Gamma_{\text{LO}}(M_H)} &= 1 + 0.884649 + 0.167738 - 0.0114242 - 0.0203406 - \boxed{0.00587368}.
\end{aligned}$$

8 Asymptotic Padé-Borel approximant improved $H \rightarrow gg$ decay rate

In this section, we apply the APAP formalism to the Borel transform of the FOPT expansion of the Higgs to gluons decay width. This method is found to have a better convergence, and is referred to as Padé - Borel approximant (PBA) in literature [58]. This formalism is applied to the $H \rightarrow b\bar{b}$ decay rate in reference [74]. In this work, we apply the generalized Borel transform to the perturbative expansion given in equation 7.31.

We first briefly review the formalism of the generalized Borel transform [75]. Let $\Psi(t)$ be a function given by,

$$\Psi(t) = \sum_{n=0}^{\infty} \Psi_n t^n. \quad (8.56)$$

For our purpose, $\Psi(t)$ is a comparison function restricted by auxiliary conditions $\Psi_n > 0$ and $\lim_{n \rightarrow \infty} \Psi_{n+1}/\Psi_n = 0$. We note that a comparison function $\Psi(t)$ is necessarily an entire function ensured by the ratio test of convergence. A function f is referred to as Ψ -type if there exists the following relation,

$$|f(r \exp(i\theta))| \leq M\Psi(\tau r), \quad (8.57)$$

where M and τ are some numbers. The infimum of numbers τ for which equation 8.57 holds defines the class of functions called Ψ -type τ [75]. The Ψ -type of a function can be obtained from the coefficients in its power series expansion using the Nachbin's theorem [75],

$$\text{Nachbin's theorem : A function } f(z) = \sum_{n=0}^{\infty} f_n z^n \text{ is of } \Psi\text{-type } \tau \text{ if and only if } \lim_{n \rightarrow \infty} |f_n/\Psi_n|^{1/n} = \tau. \quad (8.58)$$

Now we can define the generalized Borel transform given by,

$$B[f(z)](u) = \sum_n \frac{f_n}{\Psi_n} u^n. \quad (8.59)$$

Since the function f is Ψ -type τ , the domain of convergence of the function $B[f(z)]$ is $|u| \leq \tau$. Moreover, we can define [75],

$$f(z) = \frac{1}{2\pi i} \oint_{\Gamma} \Psi(zu) B[f(z)](u) du. \quad (8.60)$$

The standard Borel transform is recovered by $\Psi(t) = e^t$.

We define the generalized Borel transform of the perturbative expansion 7.31 as,

$$B[S](u) = \sum_n \left(\frac{d_1}{n!} + \frac{d_2}{n!^2} + \frac{d_3}{n!^3} + \frac{d_5}{n!^5} \right) R_n u^n, \quad (8.61)$$

where $d_{1,2,3,5}$ are the scheme-dependent real constants given in table 13. This is a phenomenological model in the sense that it reproduces the coefficient R_4 of the series 7.31 in particular, when the APAP formalism is applied to this Borel transform. The coefficient R_3 cannot be reproduced through the APAP formalism since there are three unknowns A, a and b to be fixed through the two known coefficients of the $R_{1,2}$ of the series 7.31.

Schemes	d_1	d_2	d_3	d_5
$\overline{\text{MS}}$	0.5	1.5	0	1.2
OS	1	0	1.623	0
SI	0.87	0	1.6	0
miniMOM	0.68	1.5	0	1.2

Table 13: The numerical values of the constants $d_{1,2,3,5}$.

The APAP formalism is now applied to the generalized Borel transformation defined in equation 8.61. We use the $S[1, 2]$ Padé approximant to predict the coefficient R_4 , and $S[1, 3]$ $S[2, 2]$ for the coefficient R_5 . The unknown constants of the error given in equation 7.33 are chosen to be $b = -a$. Moreover, our predictions are stable for the large values of the constants a and b , such as 10^6 . This means that as the constants a and b approach a large value, our predictions become independent of these large values. This also means from equation 7.33 that the error on our predictions practically vanishes since the constant A is independent of the values of a and b for the choice $b = -a$. Thus, from equation 7.33 for very large values of a and b we have,

$$R_{N+M+1}^{\text{Padé}} = R_{N+M+1}. \quad (8.62)$$

The PBA predictions of the coefficient R_4 in the $\overline{\text{MS}}$, SI, OS, and miniMOM schemes for $n_f = 5$ flavours are given in table 14. The very first observation is the improvement of the prediction of the coefficient $T_{4,0}$ over that of the APAP predictions. This improvement continues even in the SI and OS schemes as shown in tables 15 and 16.

$\overline{\text{MS}}$	$T_{4,0}$	$T_{4,1}$	$T_{4,2}$	$T_{4,3}$	$T_{4,4}$
PBA	-559.149	15801.3	9837.78	1579.97	68.6471
Known	-453.772	15627.2	9595.85	1574.97	67.4771
$\delta T_{4,i}$	23.2%	1.1%	2.5%	0.3%	1.7%

Table 14: The PBA predictions of the coefficients R_4 in the $\overline{\text{MS}}$ scheme with errors where, $\delta T_{4,i}^{\text{PBA}} \equiv (T_{4,i}^{\text{PBA}} - T_{4,i})/T_{4,i} \times 100$ and $i = 0 - 4$.

SI	$T_{4,0}$	$T_{4,1}$	$T_{4,2}$	$T_{4,3}$	$T_{4,4}$
PBA	-1482.92	14633.4	9574.99	1562.99	69.4497
Known	-1891.18	14042.3	9217.44	1546.13	67.4771
$\delta T_{4,i}^{PBA}$	21.6%	4.2%	3.9%	1.1%	2.9%

Table 15: The PBA predictions of the coefficients R_4 in the SI scheme with errors.

OS	$T_{4,0}$	$T_{4,1}$	$T_{4,2}$	$T_{4,3}$	$T_{4,4}$
PBA	-5.1548	16851.1	10232.9	1626.21	70.7353
Known	-5.68386	16064.3	9695.27	1574.97	67.4771
$\delta T_{4,i}^{PBA}$	9.3%	4.9%	5.5%	3.3%	4.8%

Table 16: The PBA predictions of the coefficients R_4 in the OS scheme with errors.

In the case of the miniMOM scheme as well, we notice a good improvement in the prediction of the coefficient $T_{4,1}$ over the APAP prediction of the same coefficient as shown in table 17. Thus, we can conclude that the PBA formalism is performing relatively well for our perturbative expansion.

miniMOM	$T_{4,0}$	$T_{4,1}$	$T_{4,2}$	$T_{4,3}$	$T_{4,4}$
PBA	-8517.61	415.194	7204.86	1571.76	74.0561
Known	-8939.29	401.918	6130.7	1400.56	67.4771
$\delta T_{4,i}^{PBA}$	4.7%	3.3%	17.5%	12.2%	9.8%

Table 17: The PBA predictions of the coefficients R_4 in the miniMOM scheme with errors.

In table 18 we show our overall predictions of the coefficient R_4 in the four different schemes. We observe a good agreement with that of already computed values of the coefficient R_4 in the four different schemes, and conclude that the coefficient R_4 is better predicted by the PBA formalism in the $\overline{\text{MS}}$, SI and OS schemes.

Scheme	R_4	R_4^{PBA}	δR_4	δ_4^{PBA}
$\overline{\text{MS}}$	-6957.06	-6811.95	2.0 %	-1.66573×10^{-10}
SI	-7019.12	-6701.95	4.5%	-1.01454×10^{-18}
OS	-6749.84	-6775.61	0.4%	-9.31203×10^{-13}
miniMOM	-7006.54	-5929.47	15.4%	-6.74176×10^{-12}

Table 18: PBA predicted values of R_4 at $\mu = M_H$ with relative error and asymptotic error in the $\overline{\text{MS}}$, SI, OS, and miniMOM schemes.

In a similar manner, we predict the coefficient $T_{5,i}$ for $n_f = 5$ flavours and compare it to that predicted by the RGE. Our predictions for the $\overline{\text{MS}}$, SI, OS, and miniMOM schemes in tables 19-22.

\overline{MS}	$T_{5,0}$	$T_{5,1}$	$T_{5,2}$	$T_{5,3}$	$T_{5,4}$	$T_{5,5}$
PBA	-126999	11998.4	105921	40231.5	4813.81	159.693
RGE	-	15570.1	102046	38766.7	4613.1	155.197
$\delta T_{5,i}^{PBA}$	-	22.9%	3.8%	3.8%	4.4%	2.9%

Table 19: The PBA predictions of the coefficients R_5 using the $S[1|3]$ Padé approximant in the \overline{MS} scheme with errors.

SI	$T_{5,0}$	$T_{5,1}$	$T_{5,2}$	$T_{5,3}$	$T_{5,4}$	$T_{5,5}$
PBA	-150441	-5962.74	113068	45018.4	5508.34	185.327
RGE	-	-3333.48	92400.3	37279.7	4530.19	155.197
$\delta T_{5,i}^{PBA}$	-	78.9%	22.4%	20.8%	21.6%	19.4%

Table 20: The PBA predictions of the coefficients R_5 using the $S[2|2]$ Padé approximant in the SI scheme with errors.

OS	$T_{5,0}$	$T_{5,1}$	$T_{5,2}$	$T_{5,3}$	$T_{5,4}$	$T_{5,5}$
PBA	-149714	12139.2	122438	45832.4	5490.66	180.862
RGE	-	20907.1	104628	39147.8	4613.1	155.197
$\delta T_{5,i}^{PBA}$	-	41.9%	17.0%	17.1%	19.0%	16.5%

Table 21: The PBA predictions of the coefficients R_5 using the $S[2|2]$ Padé approximant in the OS scheme with errors.

miniMOM	$T_{5,0}$	$T_{5,1}$	$T_{5,2}$	$T_{5,3}$	$T_{5,4}$	$T_{5,5}$
PBA	-69998	-129042	12610.1	24334	2963.44	208.129
RGE	-	-102578	9429.12	25325.4	4111.7	155.197
$\delta T_{5,i}^{PBA}$	-	25.8%	33.7%	3.9%	27.9%	34.1%

Table 22: The PBA predictions of the coefficients R_5 using the $S[2|2]$ Padé approximant in the miniMOM scheme with errors.

Scheme	R_5^{PBA}	R_5^{RGE}	δR_5^{PBA}	R_6^{PBA}	R_7^{PBA}	R_8^{PBA}	R_9^{PBA}
\overline{MS}	-100576	-104140	3.4%	-579764	3.14089×10^6	1.28987×10^8	1.55196×10^9
SI	-120962	-127255	4.9%	-927464	4.86118×10^6	3.10397×10^8	5.48341×10^9
OS	-117885	-129328	8.8 %	-893860	5.32098×10^6	3.12672×10^8	5.64975×10^9
miniMOM	12553.1	-5930.1	311.7%	785972	4.58537×10^6	-9.36415×10^7	-1.96327×10^9

Table 23: The PBA predicted values of R_{5-9} at $\mu = M_H$ and RGE predicted value of R_5 at $\mu = M_H$ with their relative error δR_5^{PBA} , where $\delta R_5^{PBA} = (R_5^{RGE} - R_5^{PBA})/R_5^{RGE} \times 100$ in the \overline{MS} , SI, OS, and miniMOM schemes.

Scheme	δ_5^{PBA}	δ_6^{PBA}	δ_7^{PBA}	δ_8^{PBA}	δ_9^{PBA}
\overline{MS}	5.70×10^{-13}	-1.67×10^{-8}	-1.67×10^{-8}	-1.67×10^{-8}	-1.67×10^{-8}
SI	-1.01×10^{-10}	-1.01×10^{-18}	-1.01×10^{-18}	-1.01×10^{-10}	-1.01×10^{-18}
OS	-9.31×10^{-19}				
miniMOM	-6.74×10^{-18}				

Table 24: The asymptotic errors for R_{5-9} in the \overline{MS} , SI, OS, and miniMOM schemes.

Scheme	$\Delta T_{5,0}$	$\Delta T_{5,1}$	$\Delta T_{5,2}$	$\Delta T_{5,3}$	$\Delta T_{5,4}$	$\Delta T_{5,5}$
\overline{MS}	16313.5	385.346	-5108.44	-1093.3	-396.599	39.7737
SI	40063.5	1485.59	-20210.4	-7997.47	-824.036	-46.1366
OS	44638.8	7713.91	-17974.7	-6184.05	-1072.69	7.41051
miniMOM	-2322.97	10541.1	-1861.61	-675.004	-377.319	-10.1734

Table 25: Difference between the APAP predictions and PBA predictions for the coefficients R_5 at $\mu = M_H$ in the \overline{MS} , SI, OS, and miniMOM schemes where $\Delta T_{5,i} = T_{5,i}^{APAP} - T_{5,i}^{PBA}$.

The predictions of the overall coefficients R_i^{PBA} with $i = 5-9$ in four different schemes are given in table 23. The predictions for the coefficients R_{6-9} are obtained using the $S[3, 2]$, $S[4, 2]$, $S[5, 2]$, $S[6, 2]$ Padé approximants, respectively in the \overline{MS} , SI, OS, and miniMOM schemes. The asymptotic errors on the predictions of the overall coefficients R_{5-9} in the \overline{MS} , SI, OS, and miniMOM schemes are extremely small, and are given in table 24. The RGE prediction of the coefficient R_5 is obtained assuming that the coefficient $T_{5,0}$ in the RGE is identical to that of the PBA.

For a conservative estimate of the coefficient R_5 , we associate the difference of the APAP and the PBA predictions of the coefficients $T_{5,i}$ as an uncertainty to the coefficient R_5 . This uncertainty is calculated by adding the errors on the coefficients $T_{5,i}$ given in table 25 in quadrature. This results in the following values of the coefficient R_5 at $\mu = M_H$,

$$\begin{aligned}
R_5^{\overline{MS}} &= -86422.1 \pm 16456.8, \\
R_5^{SI} &= -86387.5 \pm 40519.1, \\
R_5^{OS} &= -84249.7 \pm 45568.8,
\end{aligned} \tag{8.63}$$

$$R_5^{MM} = 2761.63 \pm 7238.89.$$

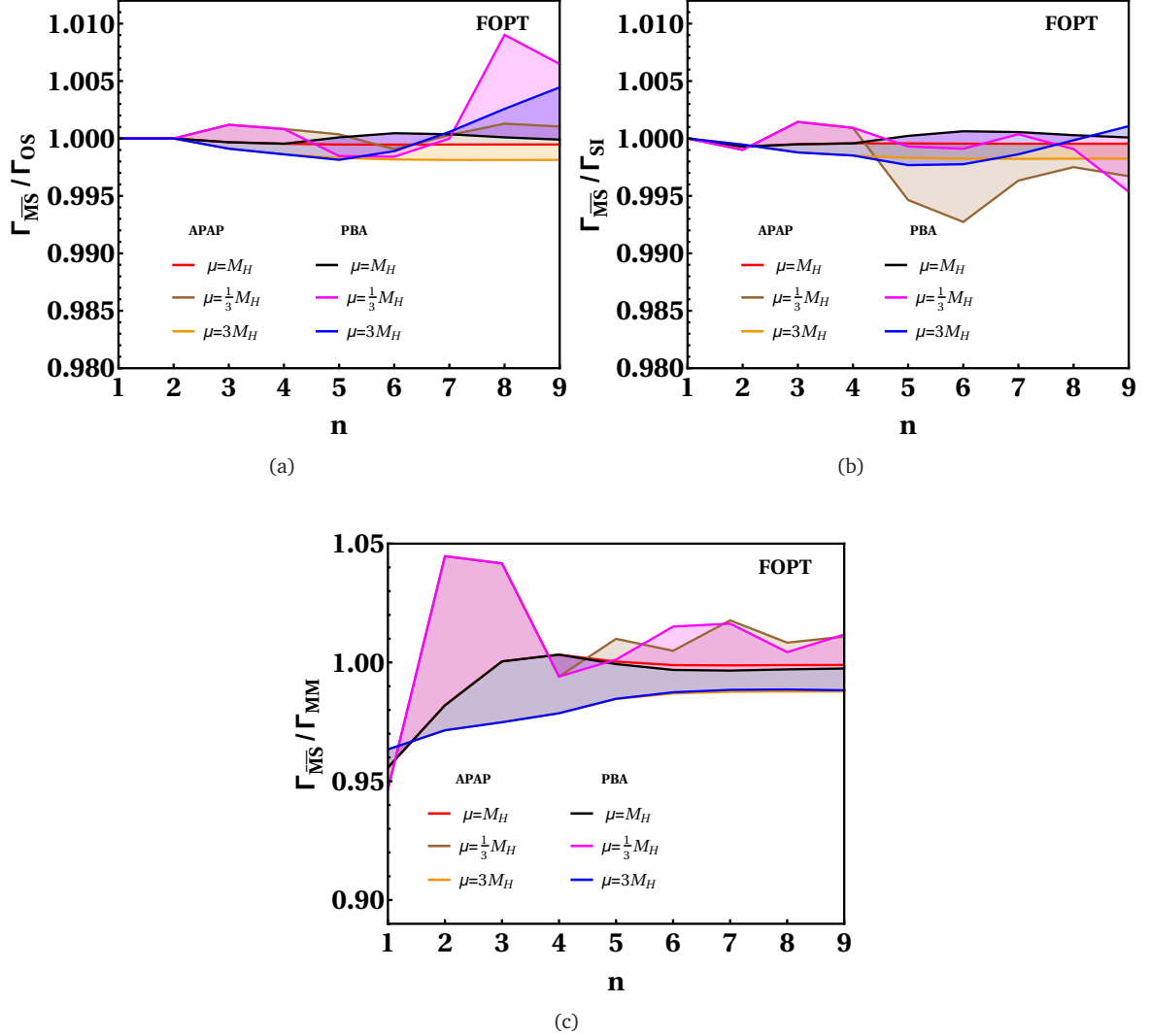


Figure 4: The variation of $\Gamma_{\overline{\text{MS}}}/\Gamma_{\text{scheme}}$ at RG scales $\mu = \frac{1}{3}M_H, M_H,$ and $3M_H$ in the FOPT in the (a)SI (b)OS and (c)miniMOM schemes up to order $n = 9$.

The higher-order behaviour of the ratio of the Higgs to gluons decay width in two different RG schemes at different orders predicted by the PBA formalism at three different RG scales in the FOPT is shown in figure 4 along with that of the APAP formalism. There is a good agreement between the predictions of the APAP and the PBA formalisms for the $\overline{\text{MS}}$, SI, and the OS schemes. We show the higher-order behaviour of the ratio of the Higgs to gluons decay width in two different RG schemes at different orders predicted by the PBA and the APAP formalisms in the RGSPT in the $\overline{\text{MS}}$, SI, OS, and miniMOM schemes in figure 5 at three different scales. As expected, the RGSPT expansions are less sensitive to the RG scale dependence.

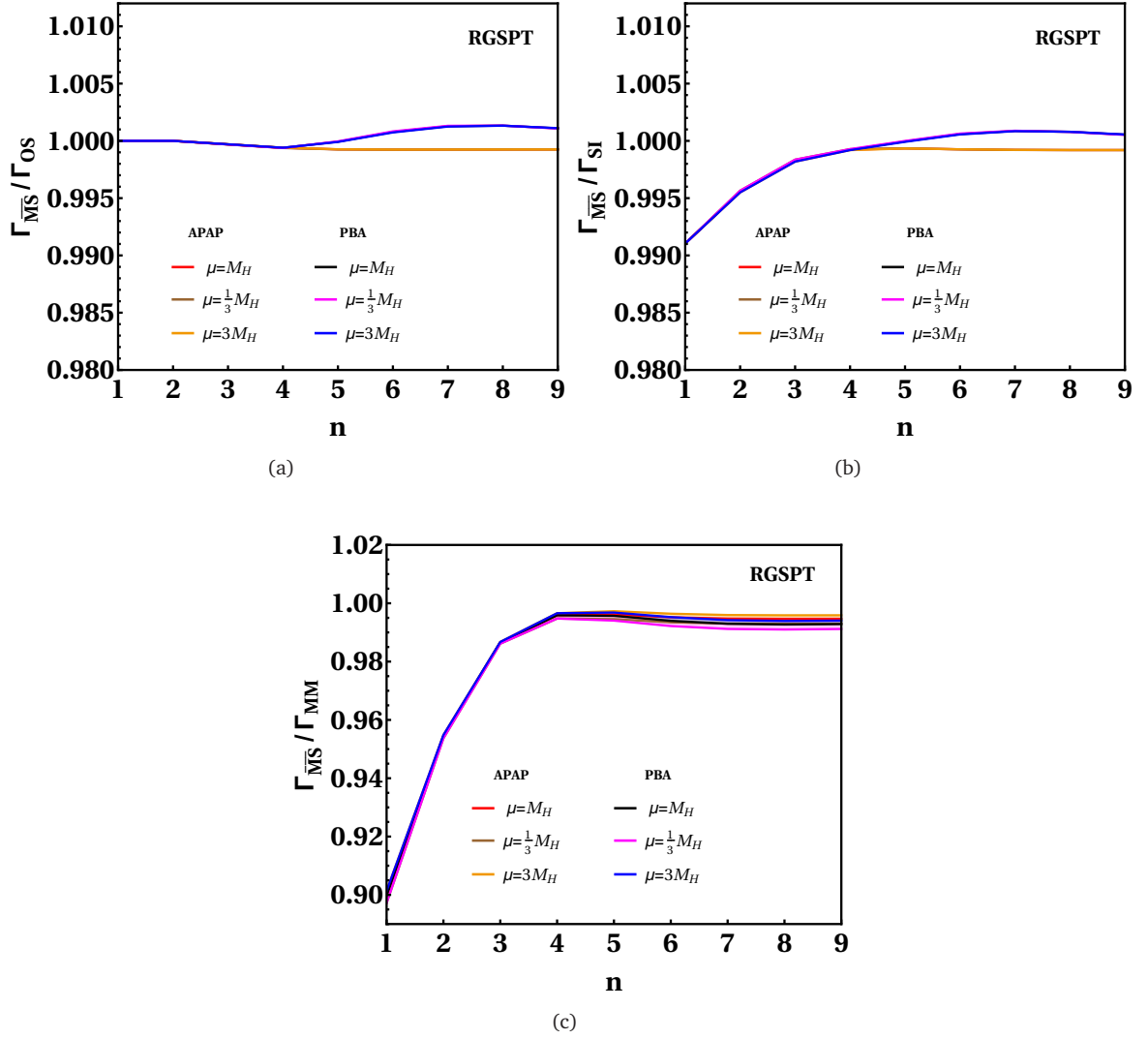


Figure 5: The variation of $\Gamma_{\overline{\text{MS}}}/\Gamma_{\text{scheme}}$ at RG scales $\mu = \frac{1}{3}M_H, M_H,$ and $3M_H$ in the RGSPT in the (a)SI (b)OS and (c)miniMOM schemes up to order $n = 9$.

We summarize our predictions using the APAP formalism using the four different RG schemes in the FOPT and in the RGSPT in figure 6. We show the the central curves of the normalised higgs to gluons decay width at RG scale $\mu = M_H$ using four different RG schemes in the FOPT on the top-left panel. On the other hand, the central curves of the ratio $\Gamma_{\overline{\text{MS}}}/\Gamma_{\text{scheme}}$ using four different RG schemes in the FOPT are shown in the top-right panel. The same curves in the RGSPT are shown in the bottom-left and the bottom-right panels. We do not show similar results in the PBA formalism due to their very similarity to the APAP predictions in the $\overline{\text{MS}}$, OS and SI schemes.

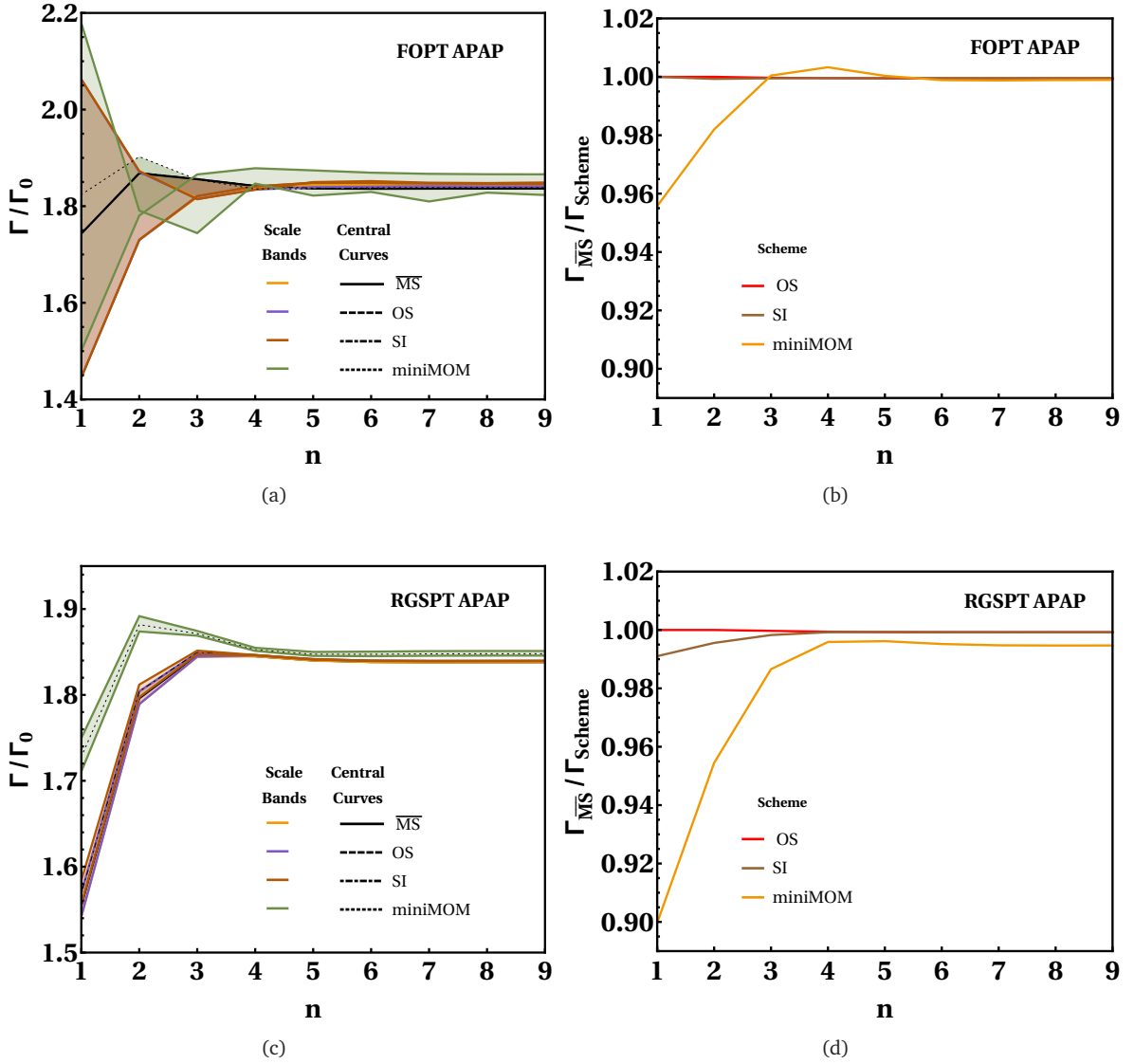


Figure 6: The variation of the normalised higgs to gluons decay width at RG scale $\mu = M_H$ with scale bands at $\mu = \frac{1}{3}M_H$ and $3M_H$ in the (a)FOFT and the (b)RGSPT in the $\overline{\text{MS}}$, SI, OS and miniMOM schemes up to order $n = 9$. The variation of $\Gamma_{\overline{\text{MS}}}/\Gamma_{\text{scheme}}$ at RG scale $\mu = M_H$ in the (b)FOFT and the (d)RGSPT in the SI, OS and miniMOM schemes up to order $n = 9$.

We now provide order-by-order perturbative evaluation of $\Gamma(H \rightarrow gg)$ decay width up to the N^5LO at $\mu = M_H$ in the FOFT using the PBA formalism. The N^5LO contribution at the scale $\mu = M_H$ is highlighted inside the box.

$$\begin{aligned} \frac{\Gamma_{PBA}^{\overline{\text{MS}}}(M_H)}{\Gamma_{LO}(M_H)} &= 1 + 0.641657 + 0.196393 + 0.0176989 - 0.0114448 - \boxed{0.00825599}, & (8.64) \\ \frac{\Gamma_{PBA}^{SI}(M_H)}{\Gamma_{LO}(M_H)} &= 1 + 0.641657 + 0.197175 + 0.0178975 - 0.0115469 - \boxed{0.00953425}, \\ \frac{\Gamma_{PBA}^{OS}(M_H)}{\Gamma_{LO}(M_H)} &= 1 + 0.641657 + 0.196393 + 0.0180594 - 0.0111039 - \boxed{0.00914739}, \end{aligned}$$

$$\frac{\Gamma_{PBA}^{MM}(M_H)}{\Gamma_{LO}(M_H)} = 1 + 0.533291 + 0.0659834 - 0.0398094 - 0.0163109 + \boxed{0.00114149}.$$

Similarly, the order-by-order perturbative evaluation of $\Gamma(H \rightarrow gg)$ decay width up to N⁵LO at $\mu = M_H$ in the RGSPT using the PBA formalism is,

$$\begin{aligned} \frac{\Gamma_{PBA}^{\overline{MS}}(M_H)}{\Gamma_{LO}(M_H)} &= 1 + 0.695577 + 0.263334 + 0.0546671 - 0.00126852 - \boxed{0.0060536}, \\ \frac{\Gamma_{PBA}^{SI}(M_H)}{\Gamma_{LO}(M_H)} &= 1 + 0.686965 + 0.253127 + 0.0487537 - 0.00318015 - \boxed{0.00739534}, \\ \frac{\Gamma_{PBA}^{OS}(M_H)}{\Gamma_{LO}(M_H)} &= 1 + 0.695577 + 0.263334 + 0.055281 - 0.000655924 - \boxed{0.00713806}, \\ \frac{\Gamma_{PBA}^{MM}(M_H)}{\Gamma_{LO}(M_H)} &= 1 + 0.884649 + 0.167738 - 0.0114242 - 0.0203406 - \boxed{0.00567677}. \end{aligned} \quad (8.65)$$

9 Determination of the Higgs to gluons decay rate

We present our predictions of the $\Gamma(H \rightarrow gg)$ decay width in the \overline{MS} , SI, OS, and miniMOM schemes in this section. The central value of the $\Gamma(H \rightarrow gg)$ decay width is evaluated at RG scale $\mu = M_H$. Assuming the $\Gamma_{N^{n+1}LO}$ approximately to be the exact result, the uncertainty due to the series expansion is estimated by the difference $(\Gamma_{N^{n+1}LO} - \Gamma_{N^n LO})/\Gamma_0$ at RG scale $\mu = M_H$. Our predictions for the $\Gamma(H \rightarrow gg)$ decay width at the order N⁵LO in the APAP formalism in the FOPT are,

$$\begin{aligned} \Gamma_{N^5LO}^{\overline{MS}} &= \Gamma_0 \left(1.837 \pm 0.047_{\alpha_s(M_Z),1\%} \pm 0.0004_{M_t} \pm 0.0066_{M_H} \pm 0.0009_P \pm 0.007_s \right), \\ \Gamma_{N^5LO}^{SI} &= \Gamma_0 \left(1.837 \pm 0.046_{\alpha_s(M_Z),1\%} \pm 0.0004_{M_t} \pm 0.0066_{M_H} \pm 0.0026_P \pm 0.007_s \right), \\ \Gamma_{N^5LO}^{OS} &= \Gamma_0 \left(1.838 \pm 0.047_{\alpha_s(M_Z),1\%} \pm 0.0004_{M_t} \pm 0.0066_{M_H} \pm 0.0023_P \pm 0.007_s \right), \\ \Gamma_{N^5LO}^{MM} &= \Gamma_0 \left(1.836 \pm 0.042_{\alpha_s(M_Z),1\%} \pm 0.0001_{M_t} \pm 0.0066_{M_H} \pm 0.0007_P \pm 0.0002_s \right), \end{aligned} \quad (9.66)$$

where P stands for the uncertainty due to the PBA predictions, and s denotes the uncertainty due to the series expansion.

Similarly, the $\Gamma(H \rightarrow gg)$ decay width using the APAP predictions at the order N⁵LO in the RGSPT are found to be,

$$\begin{aligned} \Gamma_{RGSN^5LO}^{\overline{MS}} &= \Gamma_0 \left(1.840 \pm 0.047_{\alpha_s(M_Z),1\%} \pm 0.0005_{M_t} \pm 0.0066_{M_H} \pm 0.0002_\mu \pm 0.0007_P \right), \\ \Gamma_{RGSN^5LO}^{SI} &= \Gamma_0 \left(1.841 \pm 0.047_{\alpha_s(M_Z),1\%} \pm 0.0005_{M_t} \pm 0.0066_{M_H} \pm 0.0002_\mu \pm 0.0018_P \right), \\ \Gamma_{RGSN^5LO}^{OS} &= \Gamma_0 \left(1.842 \pm 0.047_{\alpha_s(M_Z),1\%} \pm 0.0005_{M_t} \pm 0.0066_{M_H} \pm 0.0002_\mu \pm 0.0019_P \right), \\ \Gamma_{RGSN^5LO}^{MM} &= \Gamma_0 \left(1.847 \pm 0.043_{\alpha_s(M_Z),1\%} \pm 0.0005_{M_t} \pm 0.0066_{M_H} \pm 0.0023_\mu \pm 0.0002_P \right). \end{aligned} \quad (9.67)$$

We notice a few important observations in our results. The uncertainty due to the mass of the top quark in the \overline{MS} , SI and OS schemes turns out to be smaller, for instance, a change of 4 GeV in the top quark mass[76], causes 0.02% change in the $\Gamma(H \rightarrow gg)$ decay width. In the miniMOM scheme uncertainty due to the 4 GeV change in the top quark mass is 0.01% in the FOPT whereas it is 0.03% in the RGSPT. The dependence of the $\Gamma(H \rightarrow gg)$ decay width on the mass of the Higgs boson is of the order 0.36% in the \overline{MS} , SI, OS, and miniMOM scheme. The largest uncertainty in the $\Gamma(H \rightarrow gg)$ decay width at the N⁵LO originates from the change in the

strong coupling $\alpha_s(M_Z^2)$. For instance, a change of 1% in the $\alpha_s(M_Z^2)$ causes an uncertainty (2.5 – 2.6)% in the $\overline{\text{MS}}$, SI and OS schemes. For the miniMOM scheme, it is slightly less in the range (2.3 – 2.4)%.

As observed in our previous discussion, the miniMOM scheme is not showing a stable behaviour at higher orders in the APAP and PBA formalism. Therefore, excluding the prediction of this scheme, we provide our final prediction of the $\Gamma(H \rightarrow gg)$ decay width at the order N⁵LO in the FOPT as,

$$\Gamma_{\text{N}^5\text{LO}} = \Gamma_0 \left(1.8375 \pm 0.047_{\alpha_s(M_Z),1\%} \pm 0.0004_{M_t} \pm 0.0066_{M_H} \pm 0.0036_{\text{P}} \pm 0.007_s \pm 0.0005_{sc} \right), \quad (9.68)$$

where sc shows the uncertainty introduced due to scheme dependence, and the error due to PBA, is obtained by adding the uncertainties due to PBA in the $\overline{\text{MS}}$, SI and OS schemes in quadrature.

In the RGSPT, the $\Gamma(H \rightarrow gg)$ decay width at N⁵LO is,

$$\Gamma_{\text{RGSN}^5\text{LO}} = \Gamma_0 \left(1.841 \pm 0.047_{\alpha_s(M_Z),1\%} \pm 0.0005_{M_t} \pm 0.0066_{M_H} \pm 0.0002_{\mu} \pm 0.0027_{\text{P}} \pm 0.001_{sc} \right). \quad (9.69)$$

10 Summary

In this work, we have investigated an important issue of the renormalization scale and scheme dependence of the $\Gamma(H \rightarrow gg)$ decay width in the FOPT and in the RGSPT at the order N⁴LO, and beyond it. The RGSPT exploits the method of summation of all RG-accessible logarithms, which was first proposed in reference [42]. In the RGSPT, the RG equation is utilized to derive the summation of the leading and subsequent finite subleading logarithms to all orders in the perturbation theory. This results in a closed-form summation of the RG accessible leading and subsequent finite subleading logarithms. It is found that the dependence of the perturbative expansions on the RG scale μ is considerably reduced in the RGSPT expansions.

This work is motivated by a recent advancement in the computation of the $H \rightarrow gg$ decay rate in the limit of a heavy top quark and any number of massless light flavours at N⁴LO in reference [33]. We investigate the $\Gamma(H \rightarrow gg)$ decay width in four different renormalization schemes, namely, $\overline{\text{MS}}$, SI, OS, and miniMOM. We first discuss our predictions in the FOPT, and then compare these predictions to those obtained in the RGSPT. In the case of the FOPT expansions, the $\Gamma(H \rightarrow gg)$ decay width is highly sensitive to the RG scale up to the order N²LO, and stabilizes at the order N⁴LO. We observe that the summation of leading logarithms in the RGSPT expansions exhibits good stability and reduced sensitivity to RG scale μ . This is starkly obvious up to the order N²LO. The FOPT expansions begin to catch up with the behaviour of the RGSPT expansions from N³LO onward. Moreover, the RGSPT expansions show a stable behaviour in different RG schemes as well. The largest uncertainty in our predictions for the $\Gamma(H \rightarrow gg)$ decay width arises due to the 1% change in the strong coupling $\alpha_s(M_Z^2)$, and is in the range (2.5 – 2.6)% in the $\overline{\text{MS}}$, SI and OS schemes. The corresponding range in the miniMOM scheme is (2.3 – 2.4)%, which is slightly less than those obtained in the $\overline{\text{MS}}$, SI and OS schemes.

We have also estimated the higher-order effects on the $\Gamma(H \rightarrow gg)$ decay width using the APAP formalism. The higher-order behaviour of the perturbative expansions is alternatively determined by the PBA formalism, and found to be reasonably in agreement with that of the APAP formalism for the $\overline{\text{MS}}$, SI, and OS schemes. The $\Gamma(H \rightarrow gg)$ decay width is showing stability at higher-orders in the APAP as well as in the PBA frameworks, and it becomes less dependent on the higher-order corrections in all schemes. The RGSPT expansions continue to show greater stability against the RG scale at higher-orders in the APAP as well as in the PBA frameworks.

Finally, we provide our estimate of the $H \rightarrow gg$ decay rate at N⁵LO in the framework of the FOPT as well as the RGSPT. We have added the difference between the APAP and the PBA predictions of the $H \rightarrow gg$ decay rate at N⁵LO as an error to the final predictions of the $H \rightarrow gg$ decay rate. This uncertainty is approximately 0.19% in the FOPT, and 0.15% in the RGSPT. The uncertainty due to the truncation of series is approximately 0.6% at N⁴LO, and reduces to 0.4% at N⁵LO in the FOPT. Thus, by adding N⁵LO correction to the $H \rightarrow gg$ decay rate, the truncation error is reduced by 33% at N⁵LO. The uncertainty due to the truncation is much smaller than the error introduced by the 1% uncertainty in the strong coupling constant. We notice that the uncertainty of the order 1% in the $\Gamma(H \rightarrow gg)$ decay width may not be in the reach of the LHC. However, this precision may be accessible to a future e^+e^- linear collider[77].

We emphasize that the uncertainty due to the missing higher-order effects of QCD corrections beyond N³LO is an important issue in the Higgs physics for the upcoming high-luminosity phase of the LHC [78]. This

uncertainty reveals itself in the form of scale-dependence. The uncertainty due to scale is remarkably reduced in the framework of the RGSPT, and is approximately 0.01%. Our final predictions for the $H \rightarrow gg$ decay rate at N⁵LO in the FOPT and in the RGSPT includes the uncertainty entering due to the scheme dependence, which is approximately 0.03% in the FOPT, and 0.06% in the RGSPT. This prediction is obtained by excluding the miniMOM scheme, which is not working well within the APAP and PBA formalisms, and requires further future investigation.

There are other sources of uncertainties to the $\Gamma(H \rightarrow gg)$ decay width. For instance, the electroweak corrections cause the enhancement of the $\Gamma(H \rightarrow gg)$ decay width by about 5% [79, 80, 81, 82]. The missing electroweak corrections beyond NLO introduce the residual theoretical uncertainties of the order 1% [83]. Additionally, corrections due to a finite bottom-quark mass induce a 12% effect at leading order, and 6% effect at NLO to the effective Higgs coupling to gluons [22, 23]. A comprehensive analysis of these effects in the framework of the RGSPT is beyond the scope of this paper, and will be presented in future work.

Acknowledgments

We are extremely grateful to the referee for the highly constructive feedback on this work. We are also grateful to Prof. Irinel Caprini, Prof. B. Ananthanarayan and M. S. A. Alam Khan for very important comments and suggestions on the manuscript. We are also very thankful to Prof. M. Spira for very useful comments and suggestions on the first arXiv version of the manuscript. This work is supported by the Council of Science and Technology, Govt. of Uttar Pradesh, India through the project “A new paradigm for flavour problem” no. CST/D-1301, and Science and Engineering Research Board, Department of Science and Technology, Government of India through the project “Higgs Physics within and beyond the Standard Model” no. CRG/2022/003237.

Data availability statements

The used data is explicitly quoted in the manuscript itself, and there is no need to deposit it separately.

References

- [1] G. Aad *et al.* [ATLAS Collaboration], Phys. Lett. B **716**, 1 (2012) doi:10.1016/j.physletb.2012.08.020 [arXiv:1207.7214 [hep-ex]].
- [2] CMS Collaboration, Phys. Lett. B **716**, 30 (2012).
- [3] J. R. Ellis, M. K. Gaillard and D. V. Nanopoulos, Nucl. Phys. B **106**, 292 (1976) doi:10.1016/0550-3213(76)90382-5
- [4] H. M. Georgi, S. L. Glashow, M. E. Machacek and D. V. Nanopoulos, Phys. Rev. Lett. **40** (1978) 692.
- [5] M. Spira, A. Djouadi, D. Graudenz and P. M. Zerwas, Nucl. Phys. B **453**, 17-82 (1995) doi:10.1016/0550-3213(95)00379-7 [arXiv:hep-ph/9504378 [hep-ph]].
- [6] T. Inami, T. Kubota and Y. Okada, *Effective Gauge Theory and the Effect of Heavy Quarks in Higgs Boson Decay*, Z. Phys. C18 (1983) 69
- [7] S.A. Larin, T. van Ritbergen and J.A.M. Vermaseren, *The large top quark mass expansion for Higgs boson decays into bottom quarks and into gluons*, Phys. Lett. B362 (1995) 134, hep-ph/9506465
- [8] M. Schreck and M. Steinhauser, *Higgs Decay to Gluons at NNLO*, Phys. Lett. B655 (2007) 148, arXiv:0708.0916
- [9] M. Krämer, E. Laenen and M. Spira, *Soft gluon radiation in Higgs boson production at the LHC* Nucl. Phys. B **511** (1998) 523, hep-ph/9611272

- [10] K.G. Chetyrkin, B.A. Kniehl and M. Steinhauser, *Decoupling relations to $O(\alpha_s^3)$ and their connection to low-energy theorems*, Nucl. Phys. B510 (1998) 61, hep-ph/9708255
- [11] Y. Schröder and M. Steinhauser, *Four-loop decoupling relations for the strong coupling*, JHEP 0601 (2006) 051, hep-ph/0512058
- [12] K.G. Chetyrkin, J.H. Kühn and C. Sturm, *QCD decoupling at four loops*, Nucl. Phys. B744 (2006) 121, hep-ph/0512060
- [13] B.A. Kniehl, A.V. Kotikov, A.I. Onishchenko and O.L. Veretin, *Strong-coupling constant with flavor thresholds at five loops in the \overline{MS} scheme*, Phys. Rev. Lett. 97 (2006) 042001, hep-ph/0607202
- [14] K. Chetyrkin, P. Baikov and J. Kühn, *The β -function of Quantum Chromodynamics and the effective Higgs-gluon-gluon coupling in five-loop order*, PoS LL2016 (2016) 010.
- [15] M. Gerlach, F. Herren and M. Steinhauser, JHEP **11**, 141 (2018) doi:10.1007/JHEP11(2018)141 [arXiv:1809.06787 [hep-ph]].
- [16] A. Djouadi, M. Spira and P. M. Zerwas, Phys. Lett. B **264** (1991) 440; S. Dawson, Nucl. Phys. B **359** (1991) 283; S. Dawson and R. Kauffman, Phys. Rev. D **49** (1994) 2298.
- [17] R. V. Harlander and W. B. Kilgore, Phys. Rev. D **64** (2001) 013015 and Phys. Rev. Lett. **88** (2002) 201801; C. Anastasiou and K. Melnikov, Nucl. Phys. B **646** (2002) 220; V. Ravindran, J. Smith and W. L. van Neerven, Nucl. Phys. B **665** (2003) 325; S. Marzani, R. D. Ball, V. Del Duca, S. Forte and A. Vicini, Nucl. Phys. B **800** (2008) 127.
- [18] T. Gehrmann, M. Jaquier, E. W. N. Glover and A. Koukoutsakis, JHEP **1202** (2012) 056; C. Anastasiou, C. Duhr, F. Dulat and B. Mistlberger, JHEP **1307** (2013) 003; C. Anastasiou, C. Duhr, F. Dulat, F. Herzog and B. Mistlberger, JHEP **1312** (2013) 088; W. B. Kilgore, Phys. Rev. D **89** (2014) 7, 073008; Y. Li, A. von Manteuffel, R. M. Schabinger and H. X. Zhu, Phys. Rev. D **91** (2015) 036008; C. Anastasiou, C. Duhr, F. Dulat, E. Furlan, T. Gehrmann, F. Herzog and B. Mistlberger, JHEP **1503** (2015) 091; C. Anastasiou, C. Duhr, F. Dulat, F. Herzog and B. Mistlberger, Phys. Rev. Lett. **114** (2015) 21, 212001; C. Anastasiou, C. Duhr, F. Dulat, E. Furlan, T. Gehrmann, F. Herzog, A. Lazopoulos and B. Mistlberger, JHEP **1605** (2016) 058
- [19] M. Spira, A. Djouadi, D. Graudenz and P. M. Zerwas, Nucl. Phys. B **453** (1995) 17.
- [20] D. Graudenz, M. Spira and P. M. Zerwas, Phys. Rev. Lett. **70** (1993) 1372; R. Harlander and P. Kant, JHEP **0512** (2005) 015; C. Anastasiou, S. Bucherer and Z. Kunszt, JHEP **0910** (2009) 068.
- [21] R. V. Harlander and K. J. Ozeren, Phys. Lett. B **679** (2009) 467 and JHEP **0911** (2009) 088; A. Pak, M. Rogal and M. Steinhauser, Phys. Lett. B **679** (2009) 473 and JHEP **1002** (2010) 025.
- [22] R. Mueller and D. G. Öztürk, JHEP **08**, 055 (2016) doi:10.1007/JHEP08(2016)055 [arXiv:1512.08570 [hep-ph]].
- [23] J. M. Lindert, K. Melnikov, L. Tancredi and C. Wever, Phys. Rev. Lett. **118**, no.25, 252002 (2017) doi:10.1103/PhysRevLett.118.252002 [arXiv:1703.03886 [hep-ph]].
- [24] M. A. Shifman, A. I. Vainshtein, M. B. Voloshin and V. I. Zakharov, Sov. J. Nucl. Phys. **30**, 711-716 (1979) ITEP-42-1979.
- [25] M. Spira, JHEP **10**, 026 (2016) doi:10.1007/JHEP10(2016)026 [arXiv:1607.05548 [hep-ph]].
- [26] M. Spira, Prog. Part. Nucl. Phys. **95**, 98-159 (2017) doi:10.1016/j.ppnp.2017.04.001 [arXiv:1612.07651 [hep-ph]].
- [27] A. Djouadi, M. Spira and P.M. Zerwas, *Production of Higgs bosons in proton colliders: QCD corrections*, Phys. Lett. B264 (1991) 440

- [28] K.G. Chetyrkin, B.A. Kniehl and M. Steinhauser, *Hadronic Higgs decay to order α_s^4* , Phys. Rev. Lett. 79 (1997) 353, hep-ph/9705240
- [29] P.A. Baikov and K.G. Chetyrkin, *Top Quark Mediated Higgs Boson Decay into Hadrons to Order α_s^5* , Phys. Rev. Lett. 97 (2006) 061803, hep-ph/0604194
- [30] S. Moch and A. Vogt, *On third-order timelike splitting functions and top-mediated Higgs decay into hadrons*, Phys. Lett. B659 (2008) 290, arXiv:0709.3899
- [31] J. Davies, M. Steinhauser and D. Wellmann, *Completing the hadronic Higgs boson decay at order α_s^4* , Nucl. Phys. B920 (2017) 20, arXiv:1703.02988
- [32] J. Davies, M. Steinhauser and D. Wellmann, *Hadronic Higgs boson decay at order α_s^4 and α_s^5* , PoS (DIS 2017) 295, arXiv:1706.00624
- [33] F. Herzog, B. Ruijl, T. Ueda, J. A. M. Vermaseren and A. Vogt, JHEP **08**, 113 (2017) doi:10.1007/JHEP08(2017)113 [arXiv:1707.01044 [hep-ph]].
- [34] F. A. Chishtie and V. Elias, Phys. Rev. D **64**, 016007 (2001) doi:10.1103/PhysRevD.64.016007 [arXiv:hep-ph/0012254 [hep-ph]].
- [35] C. T. Gao, X. G. Wu, X. D. Huang and J. Zeng, [arXiv:2109.11754 [hep-ph]].
- [36] J. Zeng, X. G. Wu, S. Bu, J. M. Shen and S. Q. Wang, J. Phys. G **45**, no.8, 085004 (2018) doi:10.1088/1361-6471/aace6f [arXiv:1801.01414 [hep-ph]].
- [37] V. Elias, F. A. Chishtie and T. G. Steele, J. Phys. G **26**, 1239-1254 (2000) doi:10.1088/0954-3899/26/8/311 [arXiv:hep-ph/0004140 [hep-ph]].
- [38] M.R. Ahmady, F.A. Chishtie, V. Elias, A.H. Fariborz, N. Fattahi, D.G.C. McKeon, T.N. Sherry, T.G. Steele, Phys. Rev. D **66**, 014010 (2002), arXiv:hep-ph/0203183.
- [39] M.R. Ahmady, F.A. Chishtie, V. Elias, A.H. Fariborz, D.G.C. McKeon, T.N. Sherry, A. Squires, T.G. Steele, Phys. Rev. D **67**, 034017 (2003), arXiv:hep-ph/0208025.
- [40] G. 't Hooft, Nucl. Phys. B **61**, 455-468 (1973) doi:10.1016/0550-3213(73)90376-3
- [41] J. C. Collins and A. J. Macfarlane, Phys. Rev. D **10**, 1201-1212 (1974) doi:10.1103/PhysRevD.10.1201
- [42] C.J. Maxwell, Nucl.Phys.Proc.Suppl. **86**, 74 (2000).
- [43] C.J. Maxwell and A. Mirjalili, Nucl.Phys. B**577**, 209 (2000), arXiv: hep-ph/0002204.
- [44] C.J. Maxwell and A. Mirjalili, Nucl.Phys. B**611**, 423 (2001), arXiv: hep-ph/0103164.
- [45] D. G. C. McKeon, Int. J. Theor. Phys. **37**, 817-826 (1998) doi:10.1023/A:1026620630263
- [46] G. Abbas, B. Ananthanarayan, I. Caprini and J. Fischer, Phys. Rev. D **87**, no.1, 014008 (2013) doi:10.1103/PhysRevD.87.014008 [arXiv:1211.4316 [hep-ph]].
- [47] G. Abbas, B. Ananthanarayan and I. Caprini, Phys. Rev. D **85**, 094018 (2012) doi:10.1103/PhysRevD.85.094018 [arXiv:1202.2672 [hep-ph]].
- [48] B. Ananthanarayan and D. Das, Phys. Rev. D **94**, no.11, 116014 (2016) doi:10.1103/PhysRevD.94.116014 [arXiv:1610.08900 [hep-ph]].
- [49] B. Ananthanarayan, D. Das and M. S. A. Alam Khan, Phys. Rev. D **102**, no.7, 076008 (2020) doi:10.1103/PhysRevD.102.076008 [arXiv:2007.10775 [hep-ph]].
- [50] G. Abbas, B. Ananthanarayan, I. Caprini and J. Fischer, Nucl. Part. Phys. Proc. **273-275**, 2777-2779 (2016) doi:10.1016/j.nuclphysbps.2015.10.061

- [51] G. Abbas, B. Ananthanarayan, I. Caprini and J. Fischer, Phys. Rev. D **88**, no.3, 034026 (2013) doi:10.1103/PhysRevD.88.034026 [arXiv:1307.6323 [hep-ph]].
- [52] G. Abbas, B. Ananthanarayan and I. Caprini, Mod. Phys. Lett. A **28**, 1360004 (2013) doi:10.1142/S0217732313600043 [arXiv:1306.1095 [hep-ph]].
- [53] G. Abbas, B. Ananthanarayan, I. Caprini and J. Fischer, PoS **EPS-HEP2013**, 413 (2013) doi:10.22323/1.180.0413
- [54] I. Caprini, Mod. Phys. Lett. A **28**, 1360003 (2013) doi:10.1142/S0217732313600031 [arXiv:1306.0985 [hep-ph]].
- [55] I. Caprini, J. Fischer, G. Abbas and B. Ananthanarayan, “Perturbative Expansions in QCD Improved by Conformal Mappings of the Borel Plane,” “Perturbation Theory: Advances in Research and Applications, Nova Science Publishers (2018), pp. 211-254.” [arXiv:1711.04445 [hep-ph]].
- [56] M. A. Samuel, G. Li and E. Steinfelds, Phys. Rev. D **48**, 869-872 (1993) doi:10.1103/PhysRevD.48.869
- [57] M. A. Samuel, G. w. Li and E. Steinfelds, Phys. Rev. E **51**, 3911-3933 (1995) doi:10.1103/PhysRevE.51.3911
- [58] M. A. Samuel, J. R. Ellis and M. Karliner, Phys. Rev. Lett. **74**, 4380-4383 (1995) doi:10.1103/PhysRevLett.74.4380 [arXiv:hep-ph/9503411 [hep-ph]].
- [59] J. R. Ellis, M. Karliner and M. A. Samuel, Phys. Lett. B **400**, 176-181 (1997) doi:10.1016/S0370-2693(97)00342-0 [arXiv:hep-ph/9612202 [hep-ph]].
- [60] J. R. Ellis, E. Gardi, M. Karliner and M. A. Samuel, Phys. Lett. B **366**, 268-275 (1996) doi:10.1016/0370-2693(95)01326-1 [arXiv:hep-ph/9509312 [hep-ph]].
- [61] J. R. Ellis, I. Jack, D. R. T. Jones, M. Karliner and M. A. Samuel, Phys. Rev. D **57**, 2665-2675 (1998) doi:10.1103/PhysRevD.57.2665 [arXiv:hep-ph/9710302 [hep-ph]].
- [62] K. G. Chetyrkin, Phys. Lett. B **404**, 161-165 (1997) doi:10.1016/S0370-2693(97)00535-2 [arXiv:hep-ph/9703278 [hep-ph]].
- [63] T. van Ritbergen, J. A. M. Vermaseren and S. A. Larin, Phys. Lett. B **400**, 379-384 (1997) doi:10.1016/S0370-2693(97)00370-5 [arXiv:hep-ph/9701390 [hep-ph]].
- [64] V. Elias, T. G. Steele, F. Chishtie, R. Migneron and K. B. Sprague, Phys. Rev. D **58**, 116007 (1998) doi:10.1103/PhysRevD.58.116007 [arXiv:hep-ph/9806324 [hep-ph]].
- [65] K. G. Chetyrkin and M. Steinhauser, Nucl. Phys. B **573**, 617-651 (2000) doi:10.1016/S0550-3213(99)00784-1 [arXiv:hep-ph/9911434 [hep-ph]].
- [66] K. Melnikov and T. v. Ritbergen, Phys. Lett. B **482**, 99-108 (2000) doi:10.1016/S0370-2693(00)00507-4 [arXiv:hep-ph/9912391 [hep-ph]].
- [67] L. von Smekal, K. Maltman and A. Sternbeck, *The Strong coupling and its running to four loops in a minimal MOM scheme*, Phys. Lett. B **681** (2009) 336, arXiv:0903.1696
- [68] J.A. Gracey, *Renormalization group functions of QCD in the minimal MOM scheme*, J. Phys. A **46** (2013) 225403 [Erratum *ibid.* A **48** (2015) 119501], arXiv:1304.5347
- [69] B. Ruijl, T. Ueda, J.A.M. Vermaseren and A. Vogt, *Four-loop QCD propagators and vertices with one vanishing external momentum*, JHEP **1706** (2017) 040, arXiv:1703.08532
- [70] P. A. Baikov, K. G. Chetyrkin and J. H. Kühn, JHEP **10**, 076 (2014) doi:10.1007/JHEP10(2014)076 [arXiv:1402.6611 [hep-ph]].

- [71] K. G. Chetyrkin, J. H. Kuhn and M. Steinhauser, *Comput. Phys. Commun.* **133**, 43-65 (2000) doi:10.1016/S0010-4655(00)00155-7 [arXiv:hep-ph/0004189 [hep-ph]].
- [72] P.A. Zyla et al. (Particle Data Group), *Prog. Theor. Exp. Phys.* 2020, 083C01 (2020) and 2021 update
- [73] George A. Baker Jr. (Editor), John L. Gammel (Editor) *Pade Approximant in Theoretical Physics* Elsevier Science; 1st Edition (February 26, 1970)
- [74] D. Boito, C. Y. London and P. Masjuan, *JHEP* **01**, 054 (2022) doi:10.1007/JHEP01(2022)054 [arXiv:2110.09909 [hep-ph]].
- [75] Ralph P. Boas, R. Creighton Buck, *Polynomial Expansions of Analytic Functions*; Springer-Verlag OHG. Berlin · Göttingen · Heidelberg 1958.
- [76] S. Alekhin, J. Blümlein, S. Moch and R. Placakyte, *Phys. Rev. D* **96**, no.1, 014011 (2017) doi:10.1103/PhysRevD.96.014011 [arXiv:1701.05838 [hep-ph]].
- [77] K. Fujii, C. Grojean, M. E. Peskin, T. Barklow, Y. Gao, S. Kanemura, H. D. Kim, J. List, M. Nojiri and M. Perelstein, *et al.* [arXiv:1506.05992 [hep-ex]].
- [78] M. Cepeda, S. Gori, P. Ilten, M. Kado, F. Riva, R. Abdul Khalek, A. Aboubrahim, J. Alimena, S. Alioli and A. Alves, *et al.* CERN Yellow Rep. Monogr. **7** (2019), 221-584 doi:10.23731/CYRM-2019-007.221 [arXiv:1902.00134 [hep-ph]].
- [79] G. Degrossi and F. Maltoni, *Phys. Lett. B* **600**, 255-260 (2004) doi:10.1016/j.physletb.2004.09.008 [arXiv:hep-ph/0407249 [hep-ph]].
- [80] U. Aglietti, R. Bonciani, G. Degrossi and A. Vicini, [arXiv:hep-ph/0610033 [hep-ph]].
- [81] S. Actis, G. Passarino, C. Sturm and S. Uccirati, *Phys. Lett. B* **670**, 12-17 (2008) doi:10.1016/j.physletb.2008.10.018 [arXiv:0809.1301 [hep-ph]].
- [82] S. Actis, G. Passarino, C. Sturm and S. Uccirati, *Nucl. Phys. B* **811**, 182-273 (2009) doi:10.1016/j.nuclphysb.2008.11.024 [arXiv:0809.3667 [hep-ph]].
- [83] A. Denner, S. Heinemeyer, I. Puljak, D. Rebuszi and M. Spira, *Eur. Phys. J. C* **71**, 1753 (2011) doi:10.1140/epjc/s10052-011-1753-8 [arXiv:1107.5909 [hep-ph]].